NASA TECHNICAL MEMORANDUM

NASA TM X-1065

EFFECTS OF WING PLANFORM ON THE AERODYNAMIC CHARACTERISTICS OF A WING-BODY-TAIL MODEL AT MACH NUMBERS 1.57, 2.16, AND 2.87

by Royce L. McKinney and Lloyd S. Jernell

Langley Research Center
Langley Station, Hampton, Va.

NATIONAL AERONAUTICS AND SPACE ADMINISTRATION • WASHINGTON, D. C. • MARCH 1965

[redacted]

NASA TM X-1065

DECLASSIFIED.
AUTHORITY. US 663
DROBKA TO LEBOW MEMO DATED.
JAN.10, 1966

EFFECTS OF WING PLANFORM ON THE AERODYNAMIC CHARACTERISTICS OF A WING-BODY-TAIL MODEL AT MACH NUMBERS 1.57, 2.16, AND 2.87

By Royce L. McKinney and Lloyd S. Jernell

Langley Research Center
Langley Station, Hampton, Va.

[redacted]

[redacted]

NATIONAL AERONAUTICS AND SPACE ADMINISTRATION

[redacted]

[redacted]

EFFECTS OF WING PLANFORM ON THE AERODYNAMIC CHARACTERISTICS OF A WING-BODY-TAIL MODEL AT MACH NUMBERS 1.57, 2.16, AND 2.87*

By Royce L. McKinney and Lloyd S. Jernell
Langley Research Center

SUMMARY

[redacted] 27042

An investigation has been made in the Langley Unitary Plan wind tunnel to determine the effects of a series of wing leading- and trailing-edge modifications on the longitudinal and lateral aerodynamic characteristics of a swept-wing configuration. The tests were conducted at Mach numbers of 1.57, 2.16, and 2.87 and at a Reynolds number of 3×10^6 per foot. The results indicate that progressively filling in the wing trailing-edge notch improved the pitching-moment linearity and decreased the center-of-pressure shift with Mach number. Adding either leading- or trailing-edge extensions to the basic wing resulted in an increase in maximum lift-drag ratio. An abrupt nonlinear variation of effective dihedral with angle of attack that occurred for the wings with large trailing-edge cutouts was essentially eliminated when the trailing-edge notch was filled in. Adding either leading- or trailing-edge extensions to the basic wing resulted in a substantial improvement in directional stability at a constant lift coefficient. [redacted]

Author 1

INTRODUCTION

The prediction of the effects of wing-planform modifications on the stability and performance of supersonic aircraft is a difficult task because of the meager amount of data available. Much of the existing information was obtained from investigations of specific aircraft with slight modifications made to cure specific problems on configurations. Preliminary investigations have been made (refs. 1 and 2) that involved systematic changes of wing planform at sweep angles of 47° and 63° and at Mach numbers up to 2; however, these tests were confined to only the longitudinal characteristics for rather limited ranges of angle of attack.

The current interest in supersonic fighter and transport aircraft in the Mach number range from about 2 to 4 creates a need for a wing-planform study in this Mach number range. Longitudinal characteristics for high angles of attack should be investigated because of the maneuverability requirements of

*Title, Unclassified.

[redacted]

fighter-type aircraft. In addition, sideslip characteristics should be determined because of the deterioration of handling qualities with increasing Mach number due to the high effective dihedral and low directional stability characteristics of many current designs.

Accordingly, a research program has been initiated at the Langley Unitary Plan wind tunnel to investigate the aerodynamic characteristics of a model with systematic changes in wing planform. The purpose of this paper is to present the results obtained from this investigation. The basic model consisted of an ogive-cylinder body with a 61.69° swept wing. Various modifications to the wing provided for two full-span leading-edge extensions having sweep angles of 64.61° and 67.01° and three trailing-edge inserts that resulted in progressively filling the trailing-edge notch until an essentially clipped delta planform was obtained. Each leading-edge extension was tested with all the trailing-edge inserts and in order to obtain the vertical-tail contribution, each resulting wing planform configuration was tested with and without a vertical tail. The tests were conducted at Mach numbers of 1.57, 2.16, and 2.87, at a constant Reynolds number of 3×10^6 per foot, at angles of attack from about -5° to 26°, and at angles of sideslip from about -2° to 10°.

SYMBOLS

The longitudinal coefficients are referred to the stability system of axes and the sideslip coefficients are referred to the body system of axes.

b	wing span, 1.667 ft
$c_{r,b}$	chord of basic wing at body center line, 0.625 ft
$\bar{c}$	mean geometric chord, ft
$\bar{c}_b$	mean geometric chord of basic wing, 0.451 ft
C_D	drag coefficient based on respective wing area, $\frac{\text{Drag}}{qS}$
$C_{D,b}$	drag coefficient based on basic wing area, $\frac{\text{Drag}}{qS_b}$
C_L	lift coefficient based on respective wing area, $\frac{\text{Lift}}{qS}$
$C_{L,b}$	lift coefficient based on basic wing area, $\frac{\text{Lift}}{qS_b}$

C_m pitching-moment coefficient based on respective wing area and computed about moment reference center of model (fig. 1), $\frac{\text{Pitching moment}}{qS\bar{c}_b}$

$C_{m,b}$ pitching-moment coefficient based on basic wing area and computed about moment reference center of model, $\frac{\text{Pitching moment}}{qS_b\bar{c}_b}$

$\left(C_{m,b}\right)'$ pitching-moment coefficient based on basic wing area and computed about a moment center yielding a 1-inch static margin, $\frac{\text{Pitching moment}}{qS_b\bar{c}_b}$

C_l rolling-moment coefficient based on respective wing area, $\frac{\text{Rolling moment}}{qSb}$

$C_{l,b}$ rolling-moment coefficient based on basic wing area, $\frac{\text{Rolling moment}}{qS_b b}$

C_n yawing-moment coefficient based on respective wing area and computed about model moment reference center, $\frac{\text{Yawing moment}}{qSb}$

$C_{n,b}$ yawing-moment coefficient based on basic wing area and computed about model moment reference center, $\frac{\text{Yawing moment}}{qS_b b}$

C_Y side-force coefficient based on respective wing area, $\frac{\text{Side force}}{qS}$

$C_{Y,b}$ side-force coefficient based on basic wing area, $\frac{\text{Side force}}{qS_b}$

C_{l_β} effective dihedral parameter based on respective wing area, $\frac{\Delta C_l}{\Delta\beta}$

C_{n_β} directional stability parameter based on respective wing area, $\frac{\Delta C_n}{\Delta\beta}$

C_{Y_β} side-force parameter based on respective wing area, $\frac{\Delta C_Y}{\Delta\beta}$

$C_{l_{\beta,b}}$	effective dihedral parameter based on basic wing area, $\frac{\Delta C_{l,b}}{\Delta\beta}$
$C_{n_{\beta,b}}$	directional stability parameter based on basic wing area, $\frac{\Delta C_{n,b}}{\Delta\beta}$
$C_{Y_{\beta,b}}$	side-force parameter based on basic wing area, $\frac{\Delta C_{Y,b}}{\Delta\beta}$
$\Delta C_{l_{\beta,b}}$	tail contribution to effective dihedral parameter, $\left(C_{l_{\beta,b}}\right)_{\text{tail on}} - \left(C_{l_{\beta,b}}\right)_{\text{tail off}}$
$\Delta C_{n_{\beta,b}}$	tail contribution to directional stability parameter, $\left(C_{n_{\beta,b}}\right)_{\text{tail on}} - \left(C_{n_{\beta,b}}\right)_{\text{tail off}}$
$\Delta C_{Y_{\beta,b}}$	tail contribution to side-force parameter, $\left(C_{Y_{\beta,b}}\right)_{\text{tail on}} - \left(C_{Y_{\beta,b}}\right)_{\text{tail off}}$
L/D	lift-drag ratio
M	Mach number
q	dynamic pressure, lb/sq ft
S	respective wing area, sq ft
S_b	basic wing area, 0.694 ft^2
V	volume
x,y	body coordinates
x_{cp}	center-of-pressure location, measured from model moment center and positive forward, in.
α	angle of attack, deg
β	angle of sideslip, deg

APPARATUS AND METHODS

Models

Details of the model are shown in figure 1. The model had an ogive nose with a cylindrical body, a wing spar, three leading- and three trailing-edge

modifications, and a vertical tail. The body had a fineness ratio of 12.5. The basic wing leading edge had a sweep angle of 61.69°. The other two leading edges provided forward extensions of the basic leading edge at the fuselage center line of approximately 33 and 67 percent $c_{r,b}$, no extension of the tip, and had sweep angles of 64.61° and 67.01°, respectively. The trailing-edge inserts provided rearward extensions of the basic trailing edge at the fuselage center line of approximately 67, 133, and 181 percent $c_{r,b}$ and tapered linearly to zero at 50, 70, and 100 percent $b/2$, respectively. The basic wing consisted of the basic leading edge attached to the wing spar, and had an airfoil section consisting of the forward one-third of the NACA 63-006 airfoil which faired into the spar and had a constant thickness from the one-third chord to the trailing edge. The same airfoil shape was used for the two other leading edges with an added slab section inserted between the spar and the forward portion described above. The trailing-edge modifications had a slab shape with a spanwise thickness distribution identical to that of the spar. The vertical tail was constructed with a constant thickness slab which had a wedge-shape leading edge and a taper ratio of about 0.514.

Tunnel

The investigation was performed in the low Mach number test section of the Langley Unitary Plan wind tunnel, which is a variable-pressure continuous-flow facility. The test section is approximately 4 feet square and 7 feet long. The nozzle leading to the test section is of the asymmetric sliding-block type which permits a continuous variation in Mach number from about 1.5 to 2.9.

Measurements, Corrections, and Tests

Aerodynamic forces and moments were measured by means of a six-component electric strain-gage balance housed within the model. The balance chamber pressure was measured for each model by means of a single static orifice located in the vicinity of the balance. The models tested included the body-alone model and the wing-body model with each of the leading-edge configurations in combination with the four trailing-edge configurations. All models were tested with and without the vertical tail. Boundary-layer transition strips 1/16 inch wide and consisting of 0.010-inch-carborundum grains imbedded in a plastic adhesive were affixed around the fuselage 0.7 inch from the nose and 0.7 inch from the leading edge of the wing and tail surfaces in a streamwise direction.

The tests were conducted at Mach numbers of 1.57, 2.16, and 2.87 and at a Reynolds number per foot of 3×10^6. The configurations were tested through an angle-of-attack range from about -3° to 26°, and through an angle-of-sideslip range from about -2° to 10°. Angles of attack and sideslip were corrected for tunnel flow angularity and for deflection of the sting and balance due to aerodynamic loads. The drag data were adjusted to correspond to free-stream static conditions in the balance chamber.

The stagnation dewpoint was maintained below -30° F to avoid tunnel condensation effects.

Wing Identification

In order to identify the various test configurations, a two-group numbering system, with associated subscripts, is used. In a combination grouping of numbers, such as in modification 67_{100}-133_{70}, the first group refers to the leading-edge extension and gives the amount of extension of the root chord in percent of $c_{r,b}$. The associated subscript gives the spanwise extent of the leading-edge modification in percent $b/2$. The second group, together with its subscript, refers to the trailing-edge insert and represents the root-chord extension in percent $c_{r,b}$ and the spanwise extent in percent $b/2$. Thus, 67_{100}-133_{70} has a 67-percent root-chord extension on the leading edge which tapers to zero at 100 percent $b/2$ and a trailing-edge insert with 133-percent root-chord extension at the center line which tapers to zero at 70 percent $b/2$.

PRESENTATION OF DATA

In order to simplify the utilization of the data, the force and moments obtained from the test have been reduced to coefficient form by using three sets of geometric constants. The resulting three types of data are based on: (1) a single wing area (the area of the basic wing) and a single moment reference center (the model moment center, fig. 1), (2) the areas of the respective wings and a single moment reference center, and (3) the wing area of the basic wing and a moment center that produces a stability margin of 1 inch for each wing and Mach number. The data are presented as follows:

DISCUSSION OF RESULTS

Longitudinal Characteristics

The data presented in figure 3 are based on the respective wing area of each configuration and therefore may be considered as basic aerodynamic data for the individual configurations. However, the lift-drag ratio (L/D) is independent of wing area and, with some reservations, this parameter can be compared for the various configurations. These data show that increasing the leading-edge sweep and/or increasing the size of the trailing-edge modifications leads to significant improvement in maximum L/D at all test Mach numbers. However, it should be kept in mind when comparing these configurations that as the wing planform is modified the center-line wing thickness ratio varies from about 0.031 to 0.008 and the fuselage-volume—wing-area parameter $V^{2/3}/S$ varies from 0.37 to 0.13 between the smallest and largest wing-area configurations. It is believed that these factors have a greater effect on L/D than the actual wing planform.

The pitching-moment data presented in figure 4 are based on the area of the basic wing and have been adjusted to provide a constant stability margin at low lift. These results indicate a considerable improvement in pitching-moment linearity as the trailing-edge insert is progressively increased until the pitch-up tendency is essentially eliminated for the full clipped-delta wing. It should be remembered that when compared on the basis of the basic wing area, a given value of lift coefficient represents a fixed weight and the wings with increased area would obtain the lift at lower angles of attack and would have lower wing loadings.

The center-of-pressure results (fig. 5) indicate that the largest trailing-edge extension provided the smallest center-of-pressure shift with Mach number, and that increasing the leading-edge sweep also tends to reduce this shift.

Lateral Characteristics

The sideslip data of figure 6 are presented to illustrate the linearity of the basic data since the lateral derivatives were obtained by using the increment in the lateral coefficients in pitch between $\beta = 0^\circ$ and $\beta = 5^\circ$. Although some nonlinearities are evident, particularly at the higher angles of attack, this method of obtaining the lateral derivatives is felt to be of sufficient accuracy. The resulting sideslip parameters are presented in figure 7 for each configuration. These data are based on respective wing geometry and the model moment reference point.

The sideslip parameters based on the basic wing geometry are summarized in figures 8 and 9 as a function of both lift coefficient and angle of attack. The results of figure 8 are for variations of leading-edge geometry with each of the trailing-edge inserts whereas the results of figure 9 are for variations of trailing-edge geometry with each of the leading-edge modifications. The

parameters are presented as a function of lift coefficient so that the effect of the reduction in wing loading due to the leading- and trailing-edge modifications may be seen. As previously mentioned, a comparison of the various configurations for a constant value of lift coefficient represents a constant weight condition and variable wing loadings. The effects noted in such a comparison are the combined effects of changing the wing planform and the required angle of attack.

The effect of leading-edge modification on the effective dihedral parameter (fig. 8(a)) indicates that the addition of the leading-edge modifications (increasing sweep) generally tends to increase the effective dihedral. The largest effects occur at the lower Mach number where the wing leading edges are subsonic. In fact, for the wings with large trailing-edge cutouts, an abrupt nonlinearity occurs in the variation of C_{l_β} with angle of attack or lift coefficient at $M = 1.57$. This nonlinearity indicates that partial wing-tip stall has probably occurred. With the full-span trailing-edge insert (figs. 8(a) and 9(a)), the panel aspect ratio is considerably reduced so that tip stall apparently does not occur and the abrupt break in $C_{l_{\beta,b}}$ is not evident. At the higher Mach numbers the effects of leading-edge sweep on $C_{l_{\beta,b}}$ are diminished and the level of effective dihedral is generally reduced as the wing leading edge becomes supersonic.

The addition of the leading-edge modifications to the wing indicates little effect on the variation of directional stability with angle of attack (fig. 8(b)) whereas filling in the trailing-edge notch generally results in a greater deterioration of $C_{n_{\beta,b}}$ with α (fig. 9(b)). However, the variation of $C_{n_{\beta,b}}$ with lift coefficient indicates a substantial improvement in the directional stability characteristics as either the leading-edge or the trailing-edge modifications are added. This improvement results from the fact that, for a constant lift, the wings having the added area (representative of a lower wing loading) can provide a given lift coefficient at a lower angle of attack and thus the detrimental effects of forebody vorticity on $C_{n_{\beta,b}}$ are delayed.

The vertical-tail contribution to the effective dihedral, directional stability, and side-force parameters are presented in figures 10, 11, and 12, respectively. The data of these figures are in terms of the basic wing area and are presented about the model moment center so that the magnitudes may be directly compared. It may be seen that the magnitude of the various vertical tail contributions are generally reduced by the addition of the trailing-edge modifications with the exception that the 67_{50} trailing edge, in some cases, increased this magnitude. The leading-edge modifications had little effect other than to slightly increase the various tail effectiveness parameters with angle of attack.

SUMMARY OF RESULTS

An investigation has been conducted to determine the effects of a series of wing leading- and trailing-edge modifications on the aerodynamic characteristics of a wing-body-tail model at Mach numbers of 1.57, 2.16, and 2.87. The results of this investigation are summarized as follows:

1. Progressively filling in the wing trailing-edge notch improved the pitching-moment linearity and decreased the center-of-pressure shift with Mach number.

2. Adding either leading- or trailing-edge extensions to the basic wing resulted in an increase in maximum lift-drag ratio.

3. An abrupt nonlinear variation of effective dihedral with angle of attack that occurred for the wings with large trailing-edge cutouts was essentially eliminated when the trailing-edge notch was filled in.

4. Adding either leading- or trailing-edge extensions to the basic wing resulted in a substantial improvement in directional stability at a constant lift coefficient.

Langley Research Center,
National Aeronautics and Space Administration,
Langley Station, Hampton, Va., November 13, 1964.

REFERENCES

1. Cooper, Morton; and Sevier, John R., Jr.: Effects of a Series of Inboard Plan-Form Modifications on the Longitudinal Characteristics of Two 47° Sweptback Wings of Aspect Ratio 3.5, Taper Ratio 0.2, and Different Thickness Distributions at Mach Numbers of 1.61 and 2.01. NACA RM L53E07a, 1953.

2. Sevier, John R., Jr.: Aerodynamic Characteristics at Mach Numbers of 1.41 and 2.01 of a Series of Cranked Wings Ranging in Aspect Ratio From 4.00 to 1.74 in Combination With a Body. NASA TM X-172, 1960.

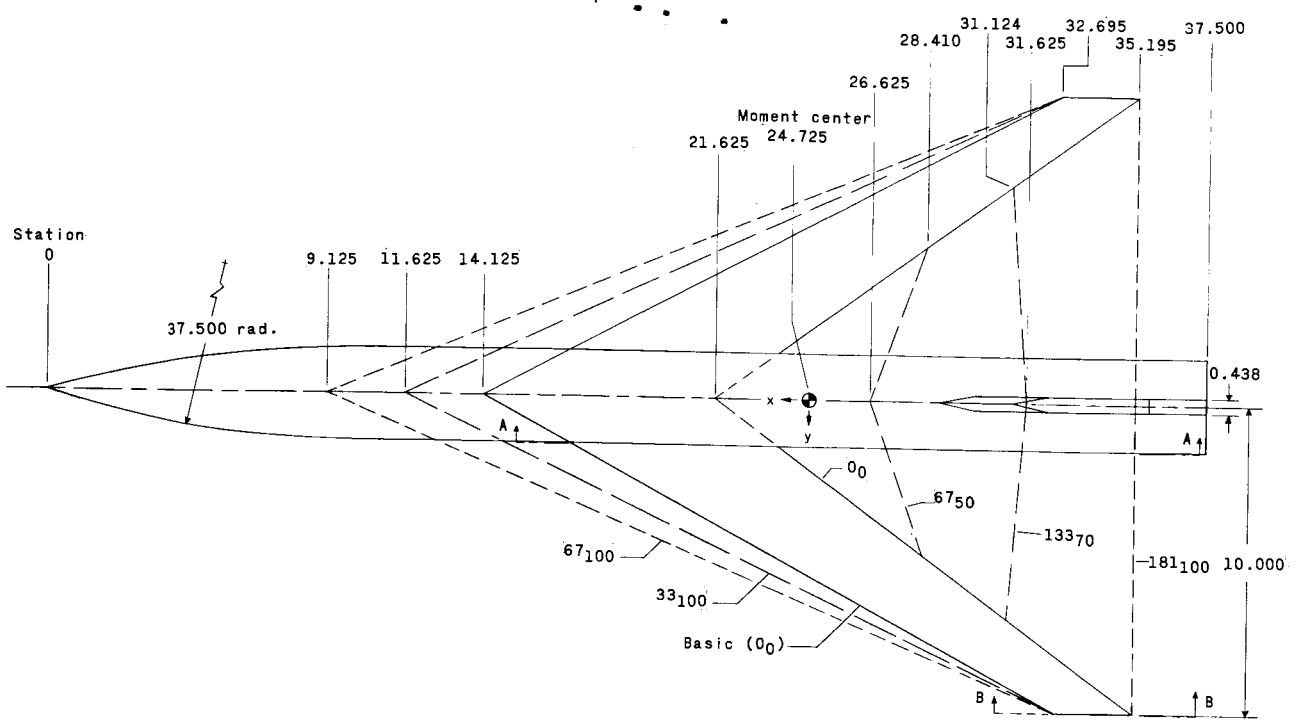

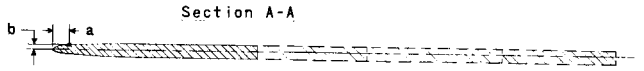

Geomtric constants for the various wings

Wing LE	Wing TE	Area, sq.ft	$\bar{c}$, in.	0.25$\bar{c}$ location x, in.	0.25$\bar{c}$ location y, in.
Basic	0	0.694	5.417	1.509	4.166
↓	5-67	.868	7.667	1.873	3.667
↓	7-133	1.180	11.127	1.477	3.411
↓	10-181	1.636	14.223	.197	3.687
10-33	0	.868	7.000	2.922	4.000
↓	5-67	1.042	9.305	3.164	3.611
↓	7-133	1.354	12.808	2.740	3.401
↓	10-181	1.810	15.873	1.434	3.653
10-67	0	1.042	8.611	4.281	3.889
↓	5-67	1.215	10.952	4.443	3.572
↓	7-133	1.528	14.462	3.985	3.394
↓	10-181	1.984	17.526	2.674	3.625

Leading-edge coordinates
Section A-A

a, in.	b, in.
0	0
.085	.052
.169	.071
.338	.099
.675	.136
1.013	.161
1.350	.179
1.688	.192
2.025	.200
2.250	.202

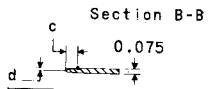

Leading-edge coordinates
Section B-B

c, in.	d, in.
0	0
.031	.019
.063	.026
.125	.037
.250	.050
.375	.060
.500	.067
.625	.071
.750	.074
.833	.075

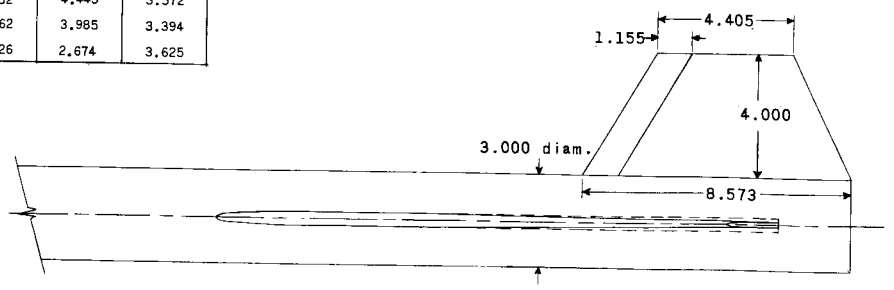

Figure 1.- Model sketch and tables of the geometric constants. (All dimensions are in inches unless otherwise noted.)

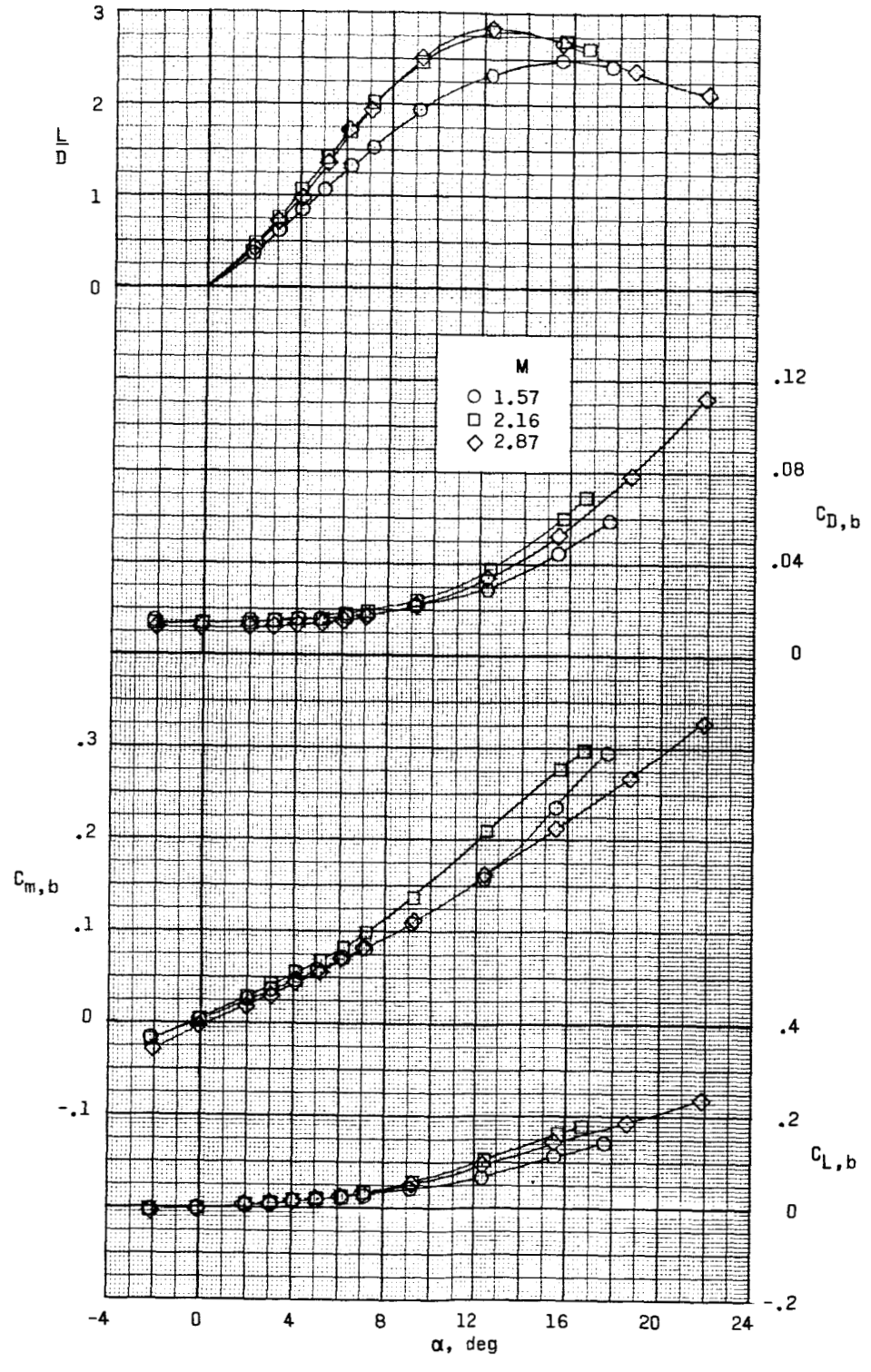

Figure 2.- Aerodynamic characteristics in pitch for body alone. (Data based on basic wing area and referenced to model moment center.)

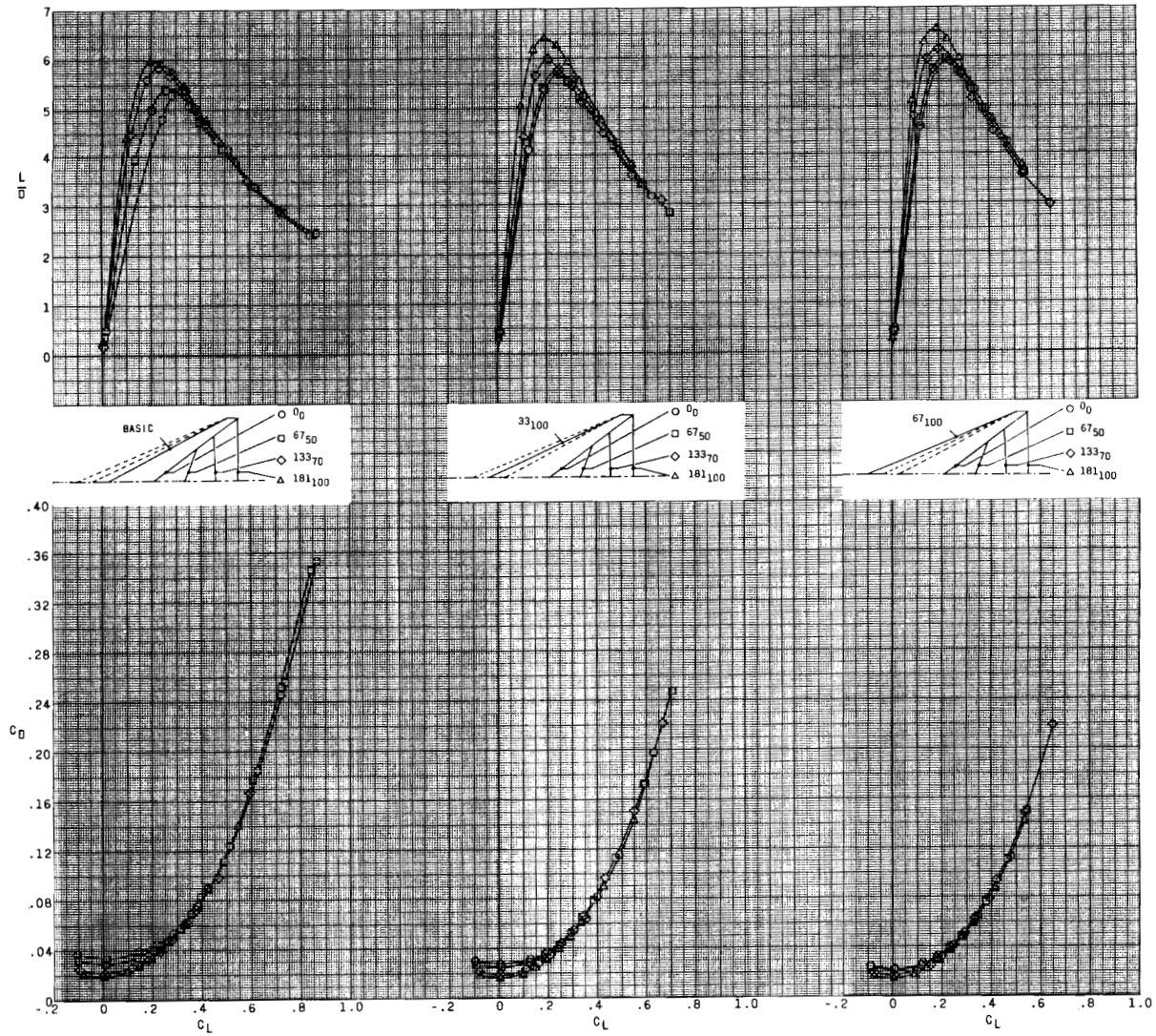

(a) M = 1.57.

Figure 3.- Aerodynamic characteristics in pitch for the various wing configurations with tail off. $\beta = 0^{\circ}$. (Data based on respective wing areas and referenced to model moment center.)

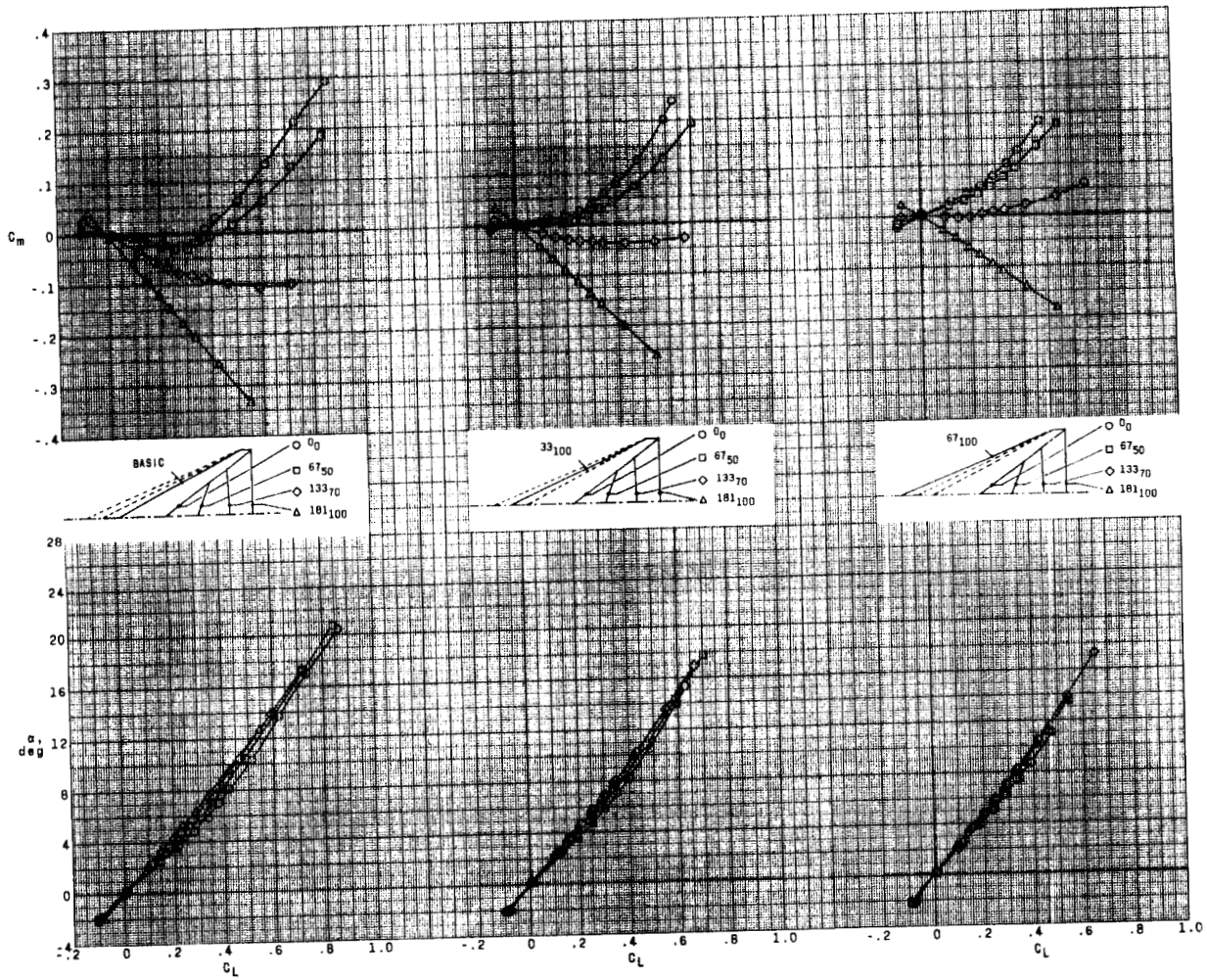

(a) M = 1.57. Concluded.

Figure 3.- Continued.

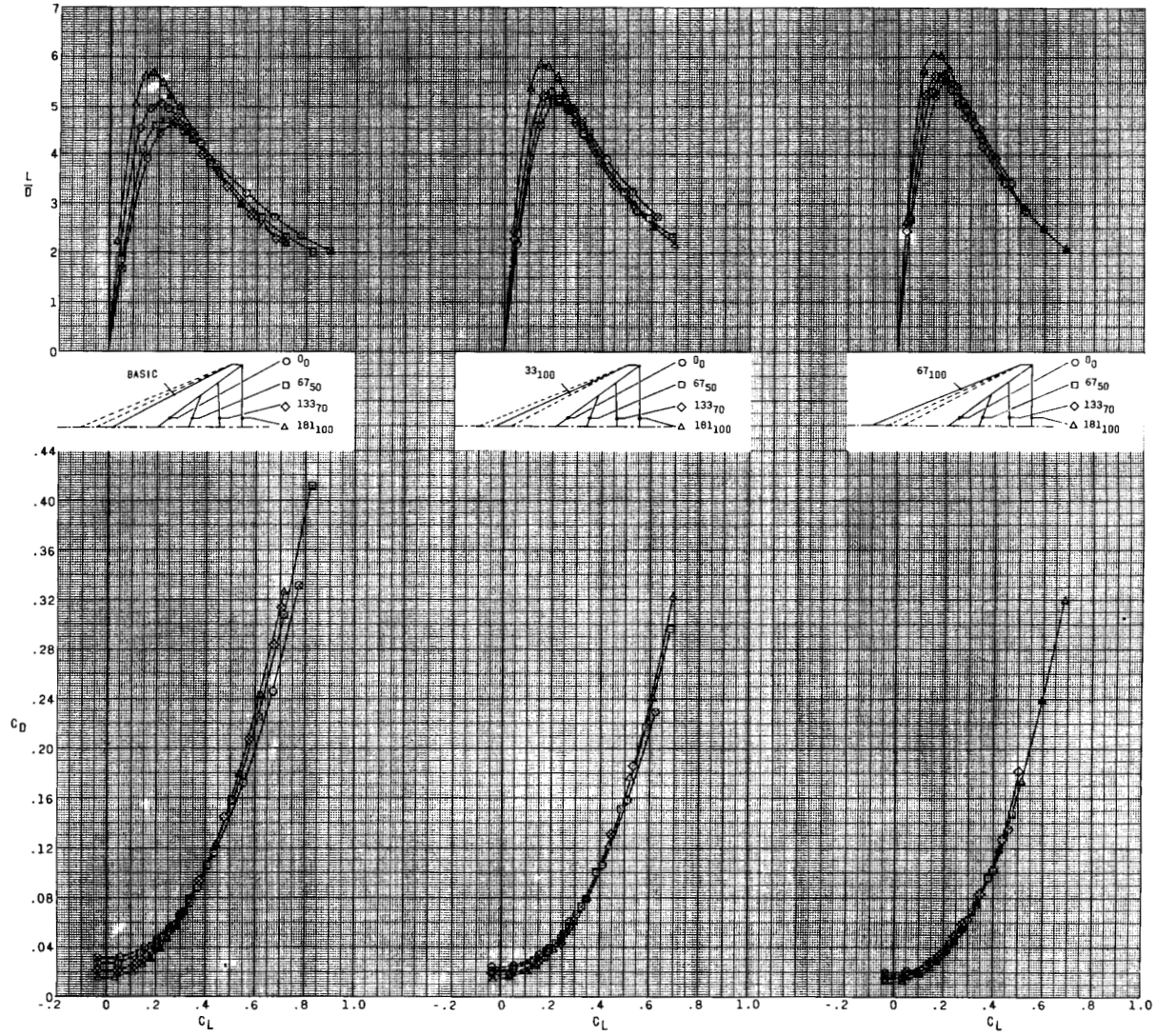

(b) M = 2.16.

Figure 3.- Continued.

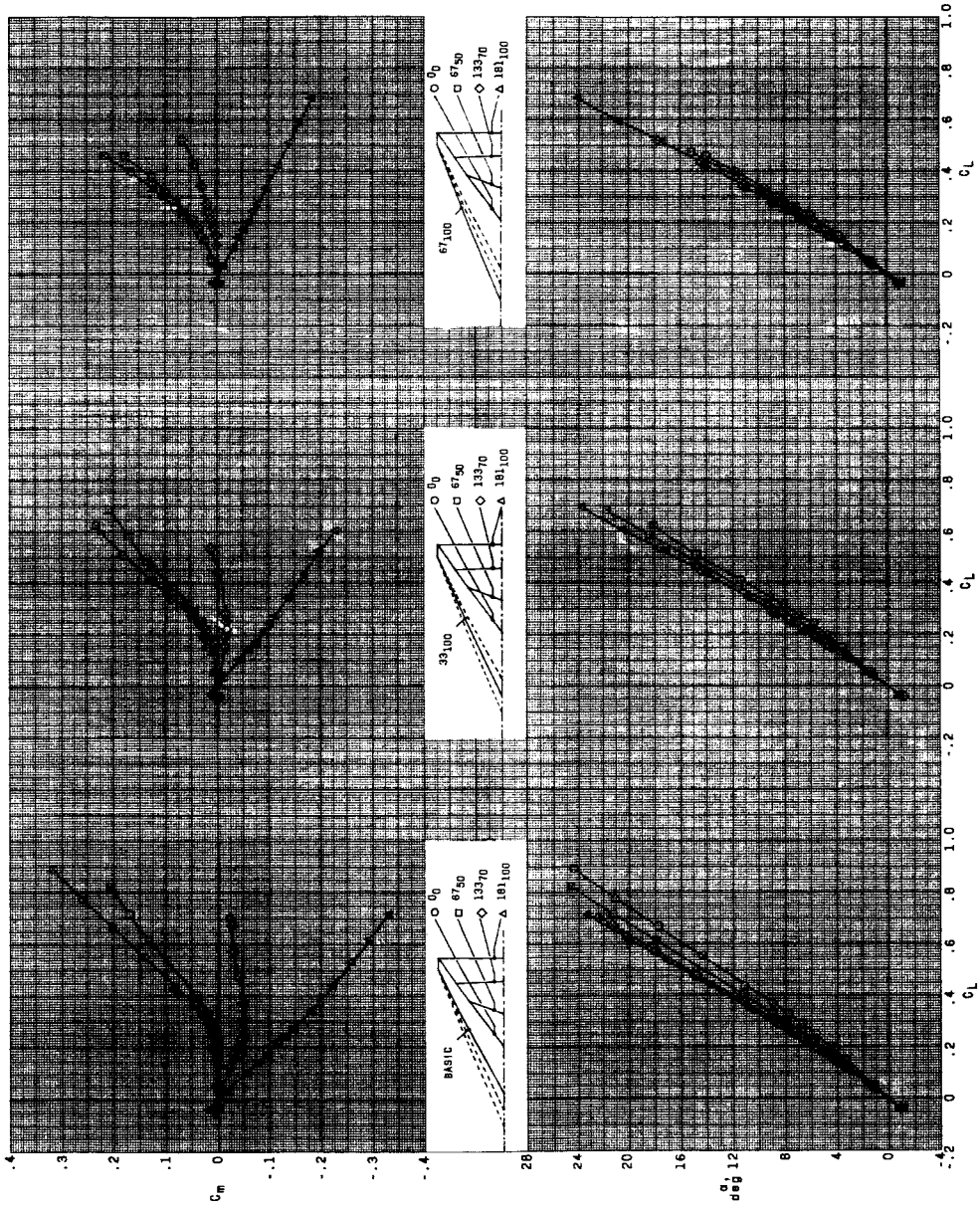

(b) M = 2.16. Concluded.

Figure 3.- Continued.

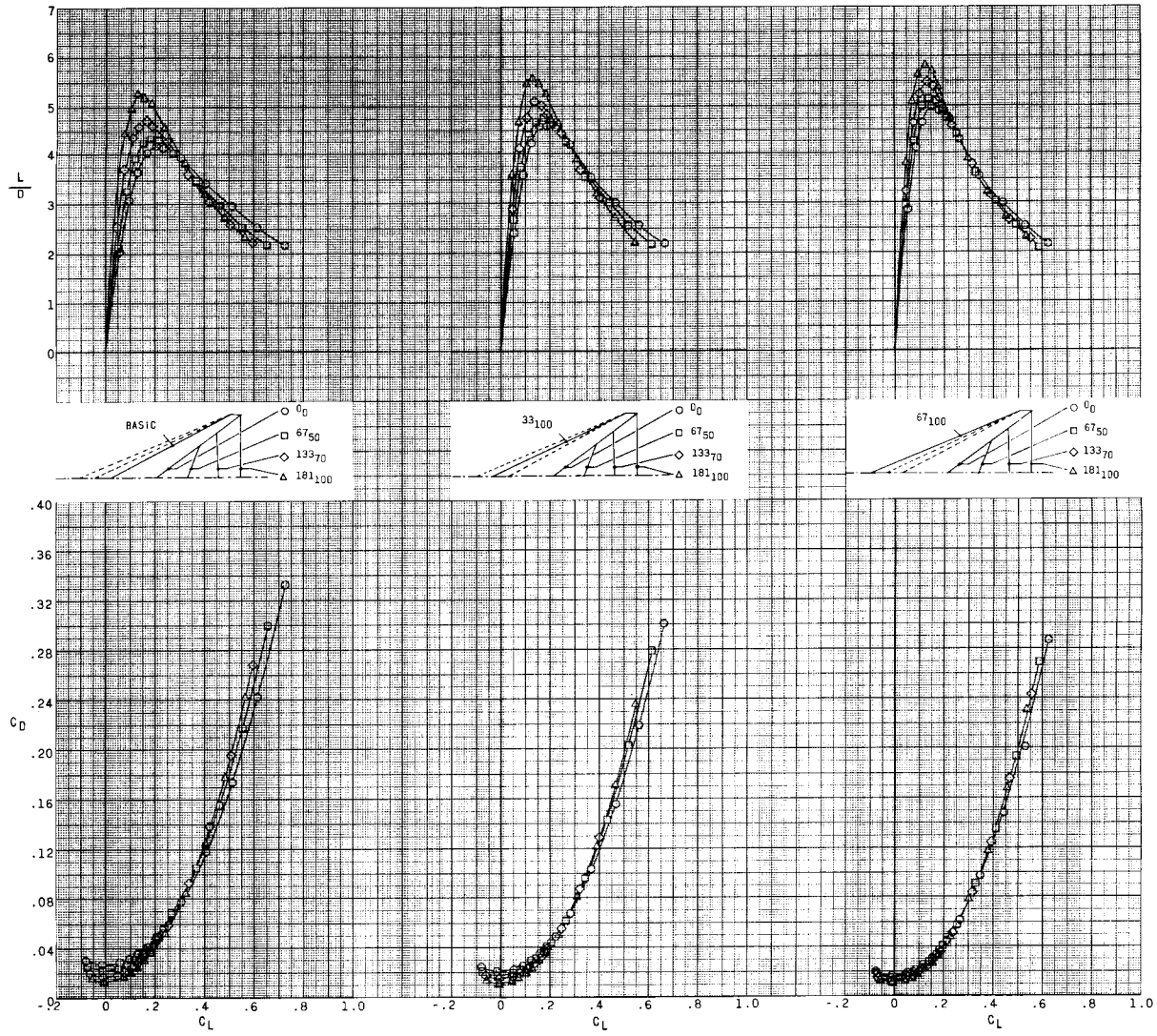

(c) M = 2.87.

Figure 3.- Continued.

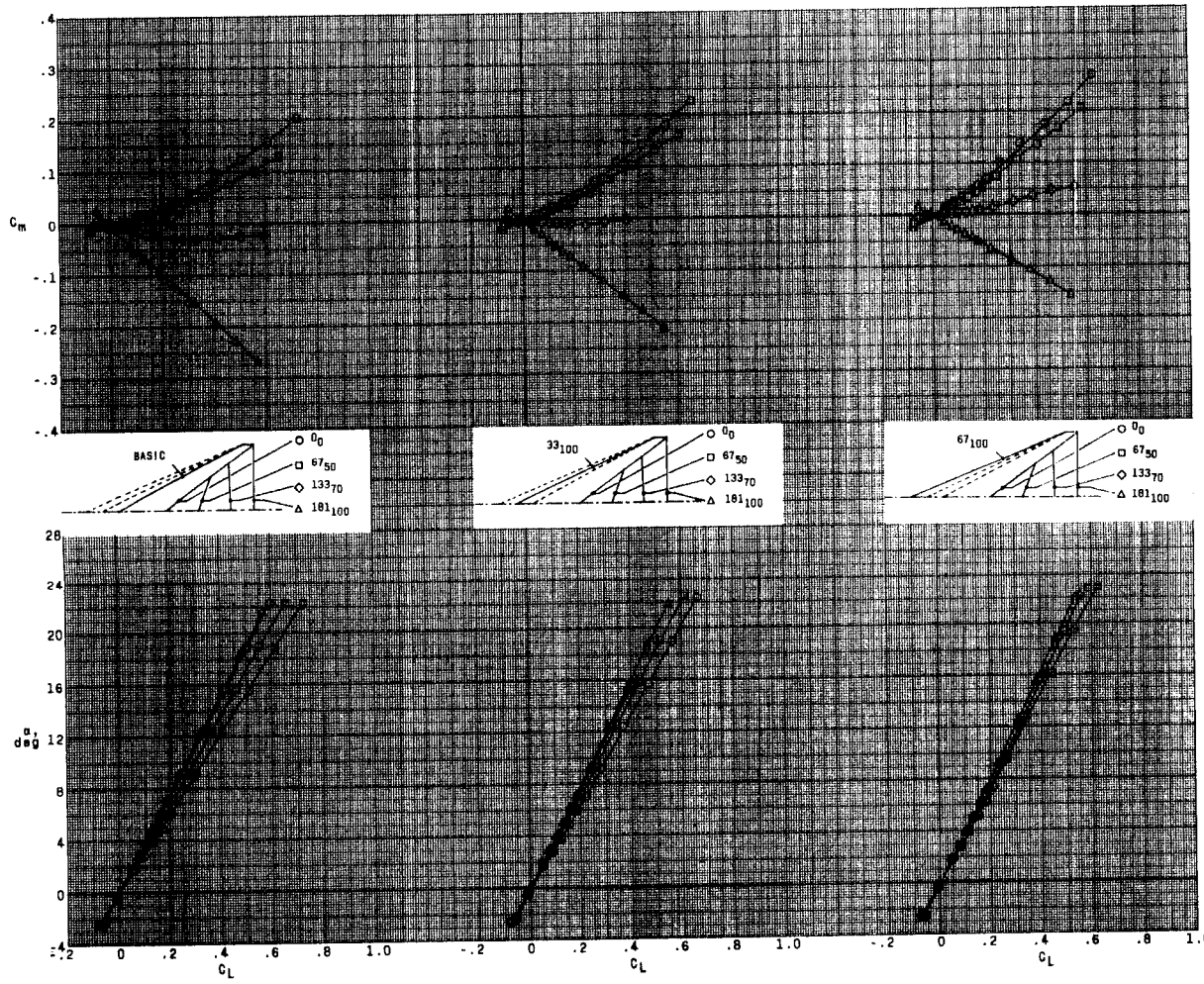

(c) M = 2.87. Concluded.

Figure 3.- Concluded.

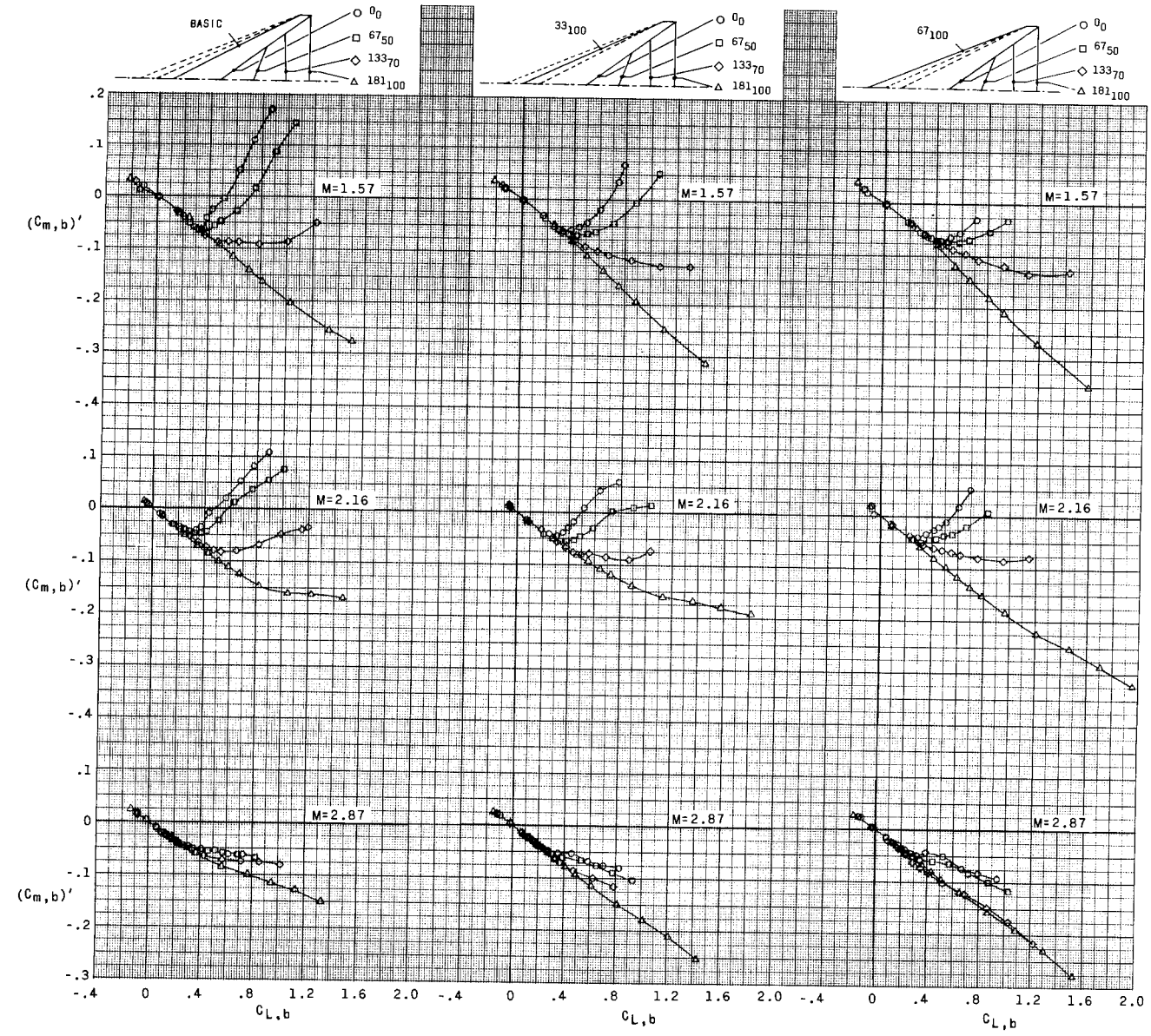

Figure 4.- Pitching-moment characteristics for the various wing configurations with tail off. $\beta = 0^{\circ}$. (Data based on basic wing area and referenced to a moment center yielding a 1-inch static margin.)

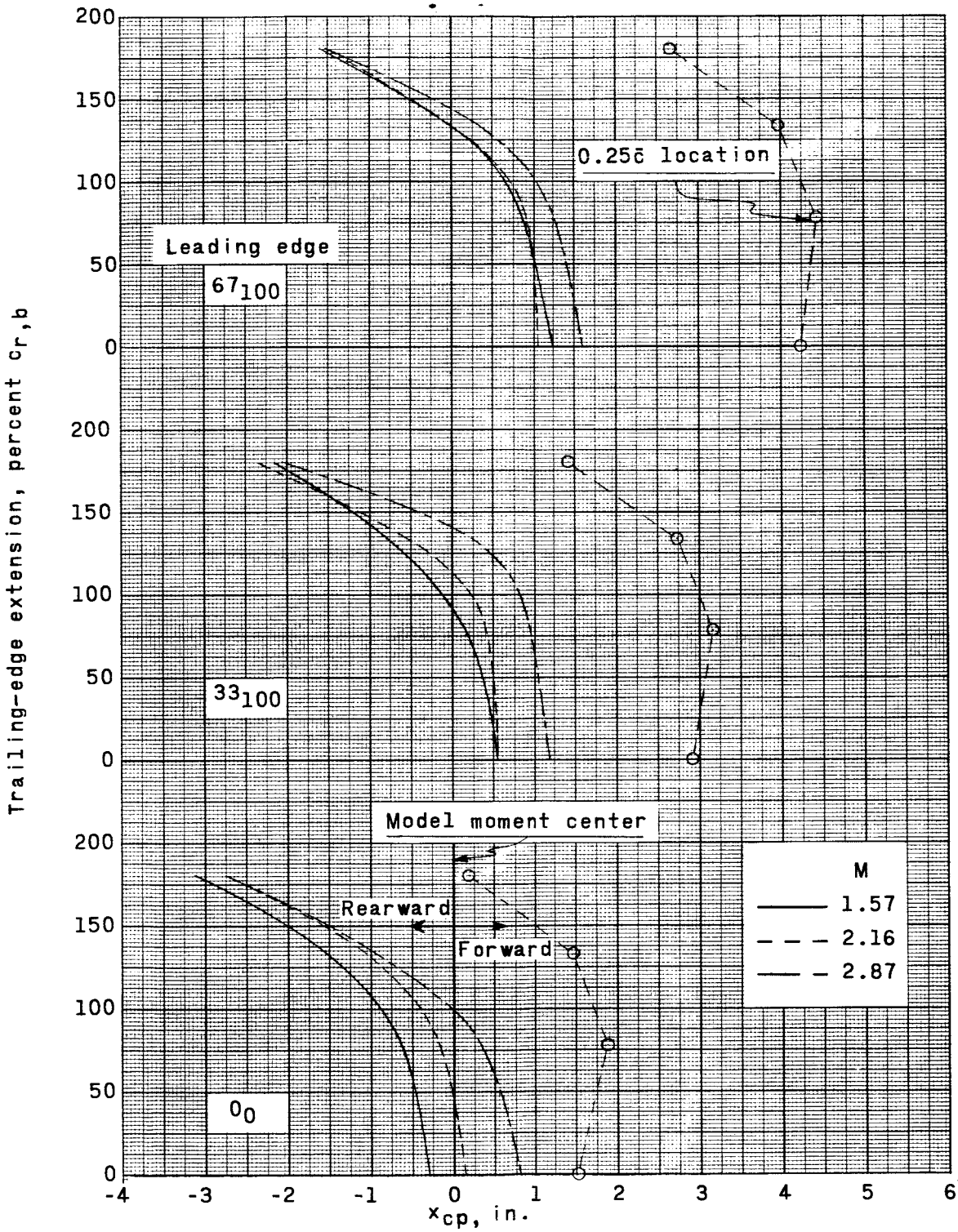

Figure 5.- Effect of wing configuration on center-of-pressure location for $C_L = 0$. Tail off.

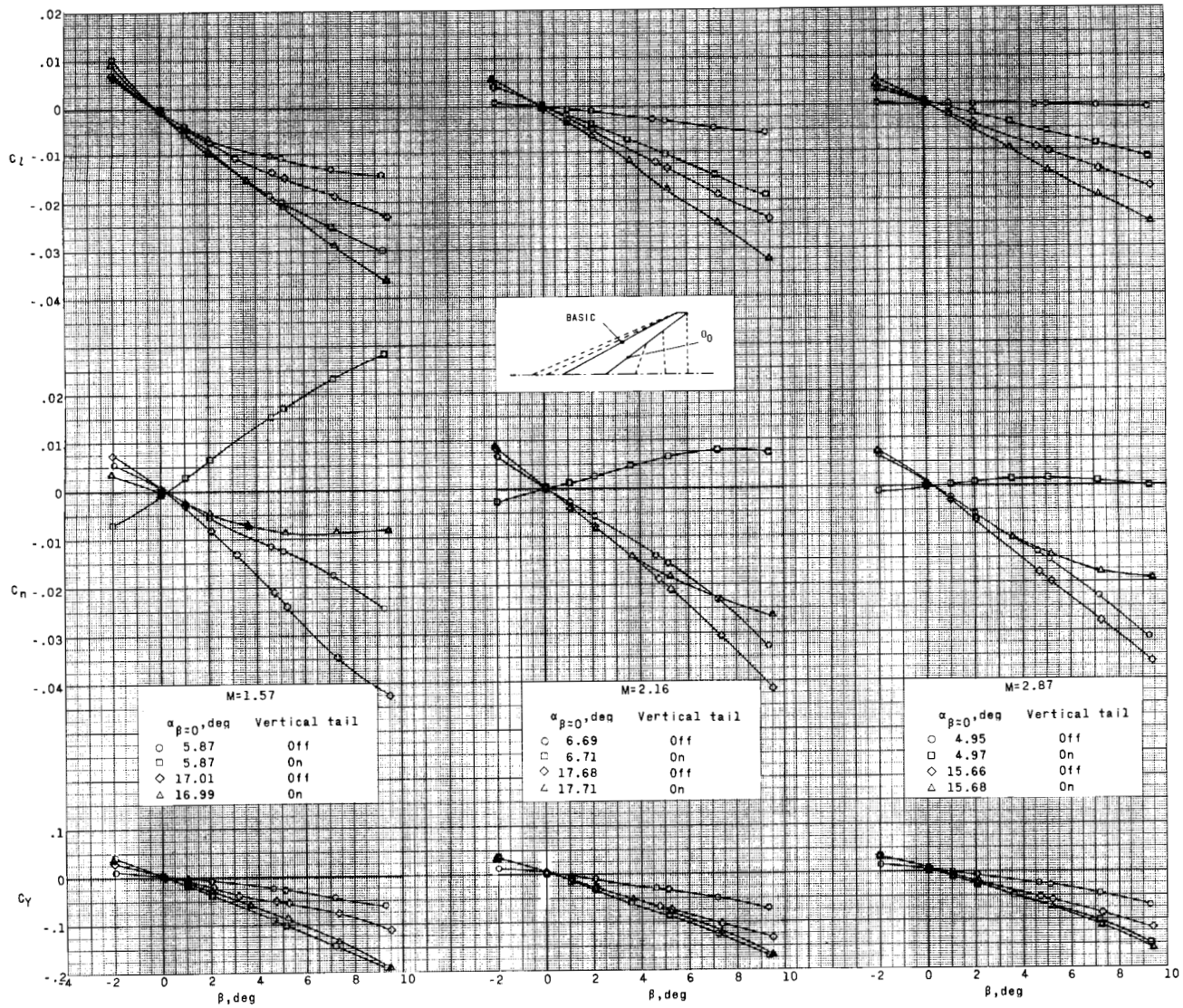

(a) Wing with smallest area.

Figure 6.- Typical aerodynamic characteristics in sideslip. (Data based on respective wing areas and referenced to model moment center.)

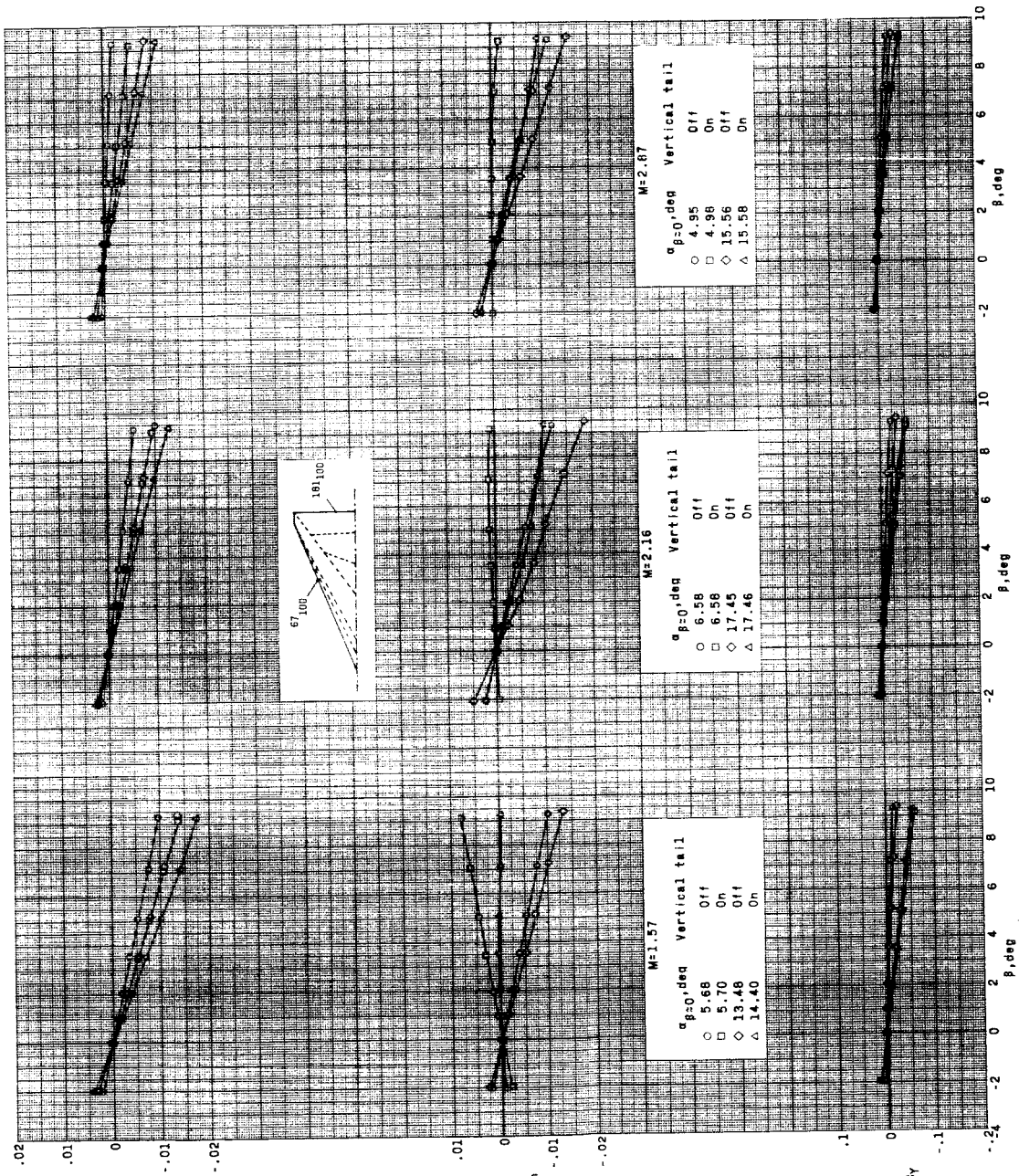

(b) Wing with largest area.

Figure 6.- Concluded.

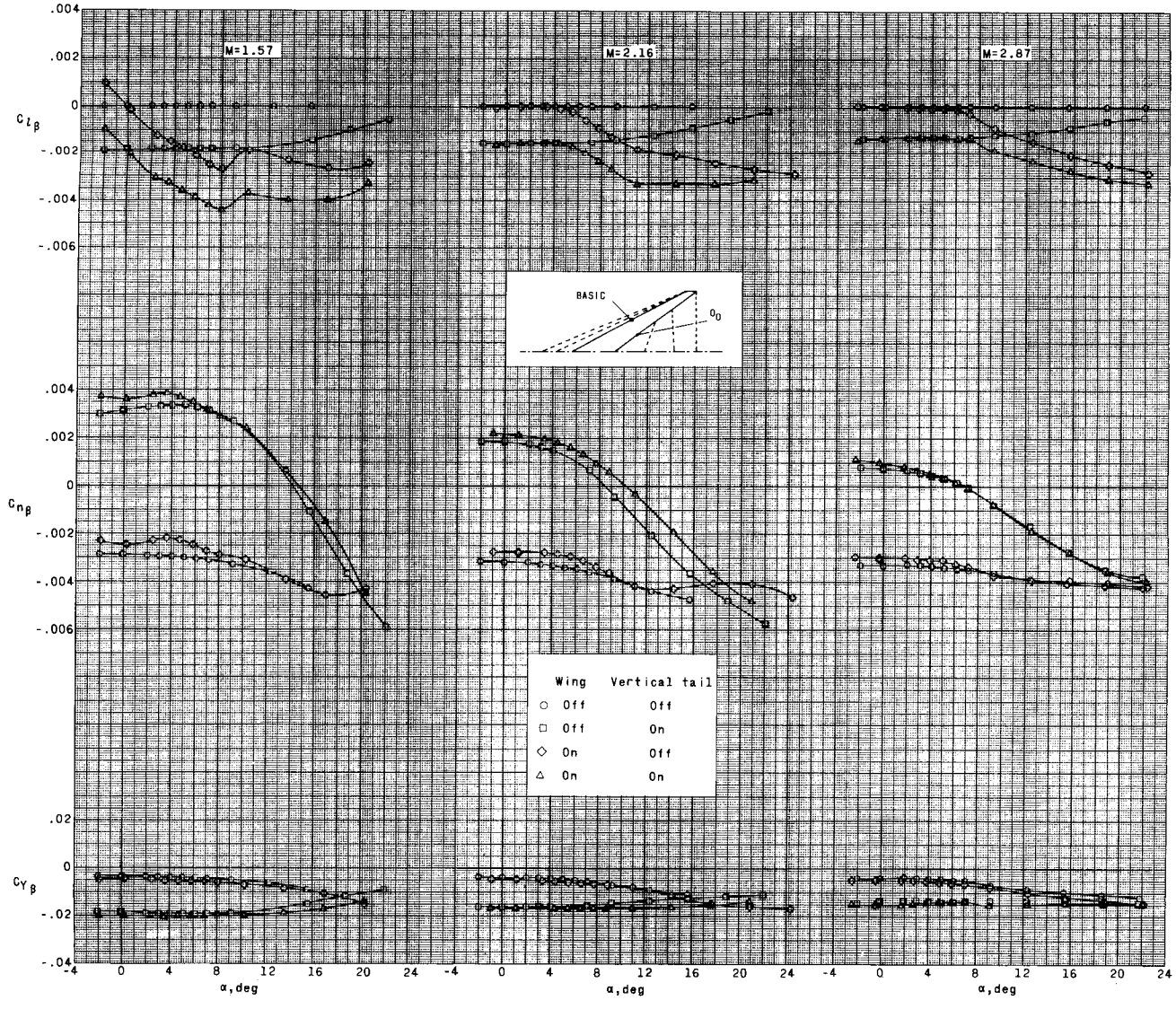

(a) 0_0-0_0.

Figure 7.- Variation of sideslip parameters with angle of attack. (Data based on respective wing areas and referenced to model moment center.)

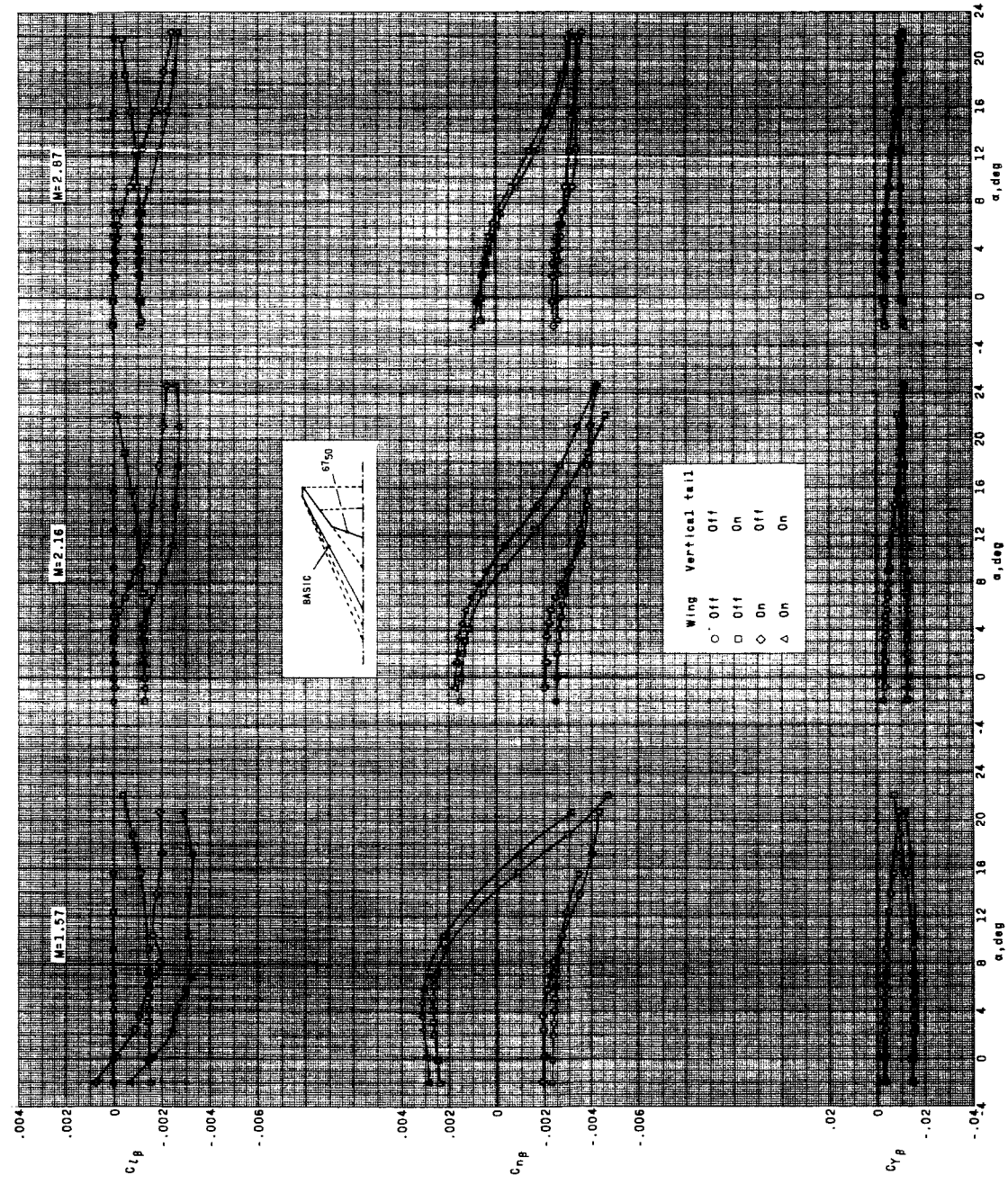

(b) 0_0-67_{50}.

Figure 7.- Continued.

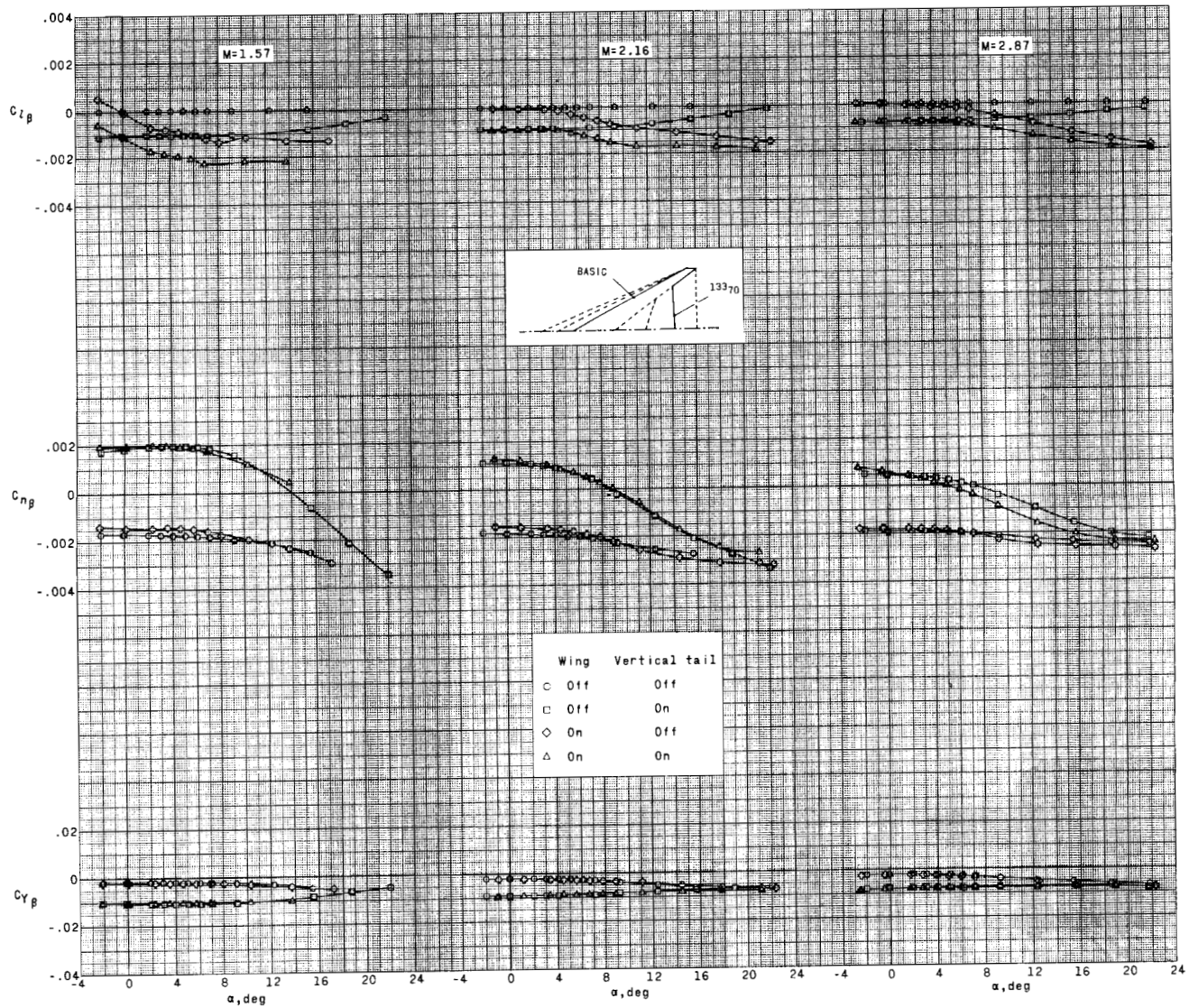

(c) 0_0-133_{70}.

Figure 7.- Continued.

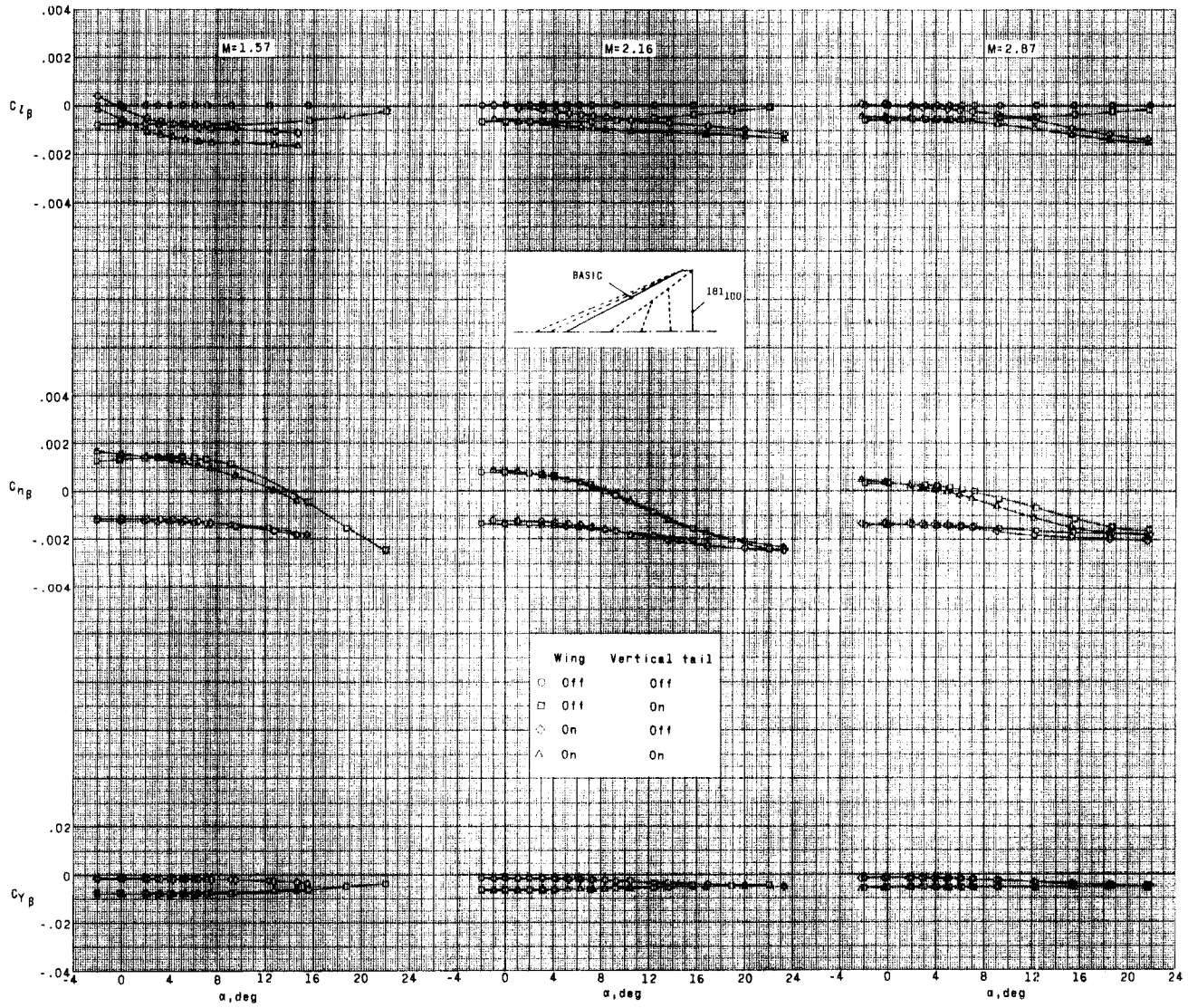

(d) 0_0-181_{100}.

Figure 7.- Continued.

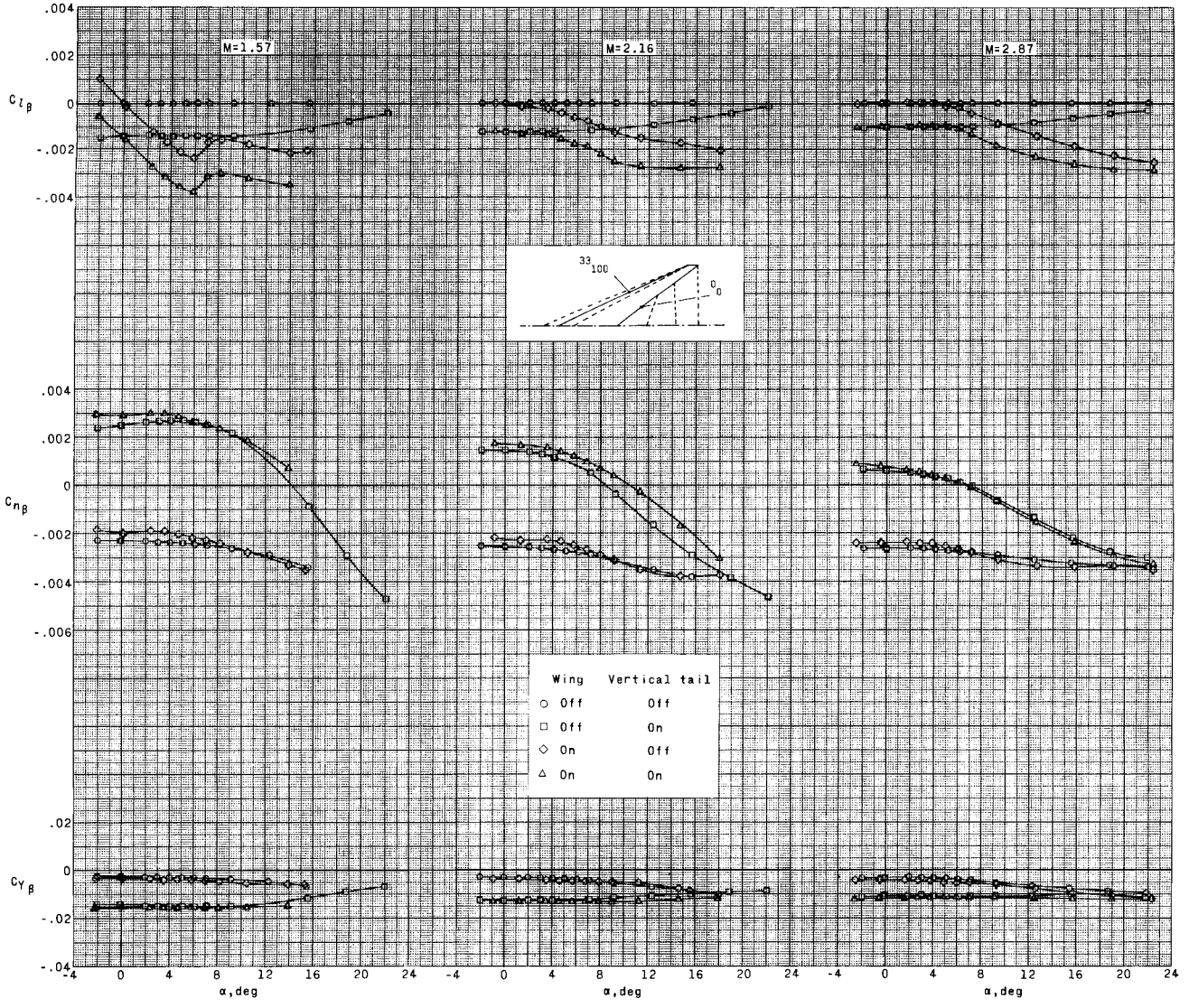

(e) 33_{100}-0_0.

Figure 7.- Continued.

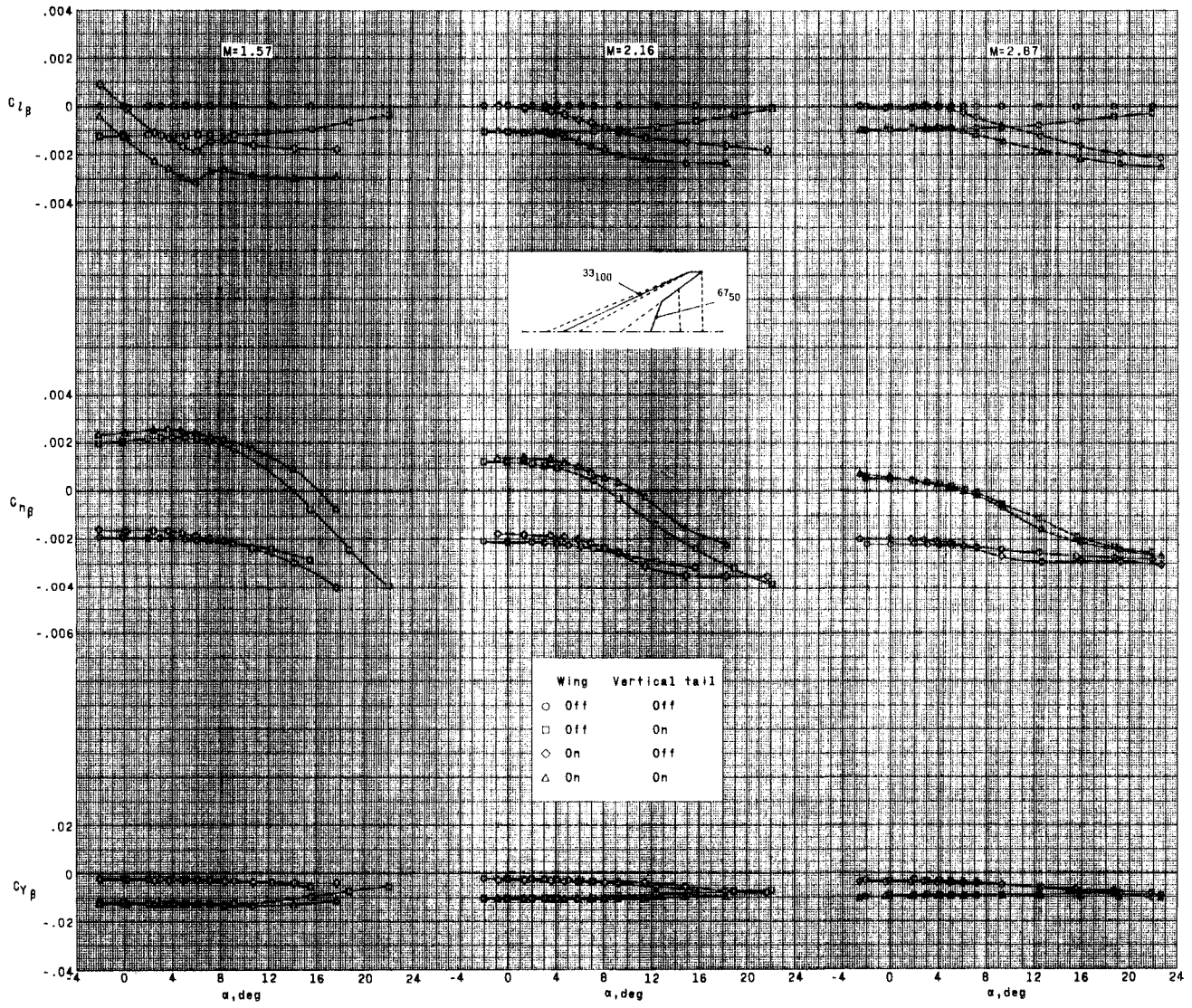

(f) 33_{100}-67_{50}.

Figure 7.- Continued.

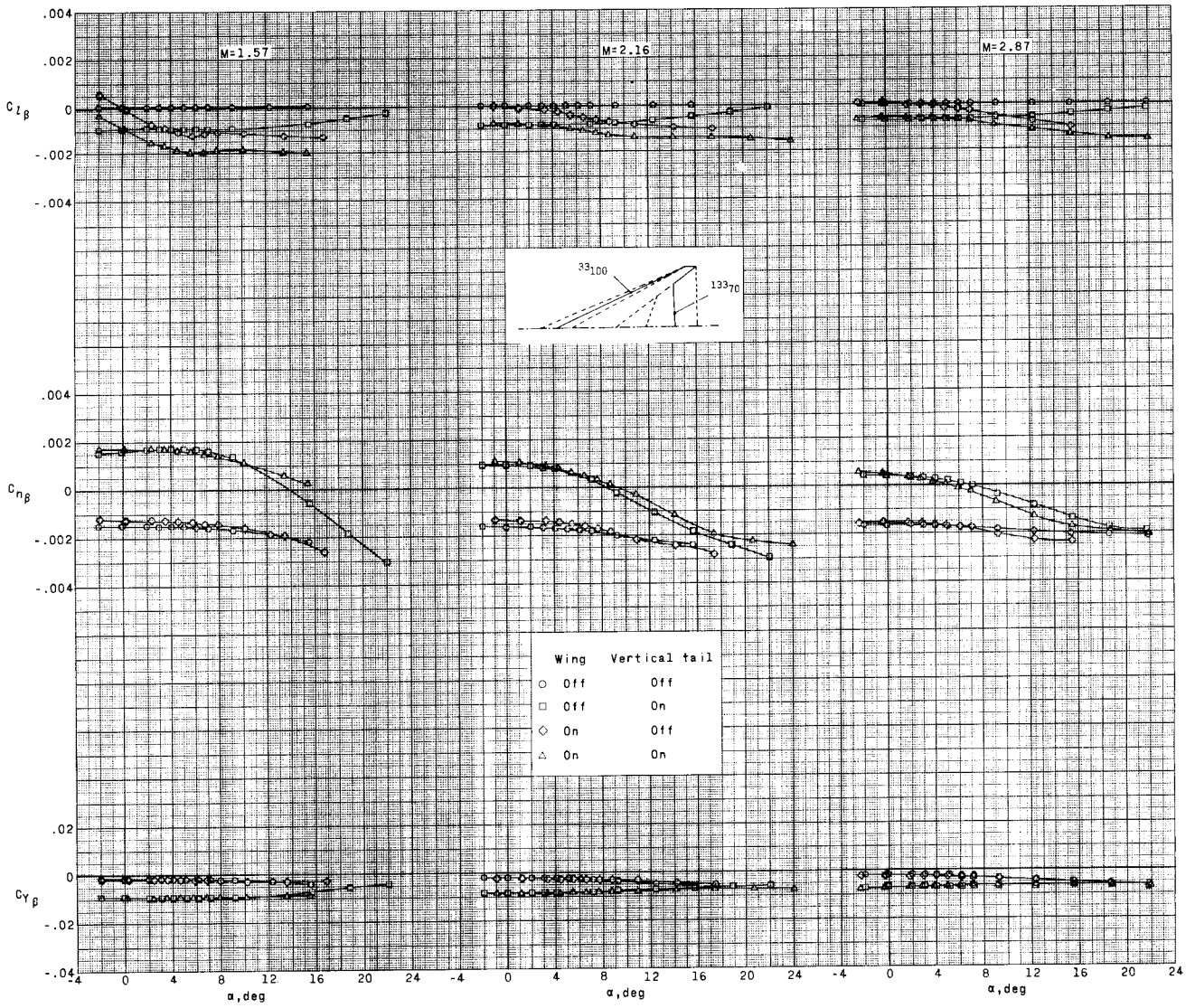

(g) 33_{100}-133_{70}.

Figure 7.- Continued.

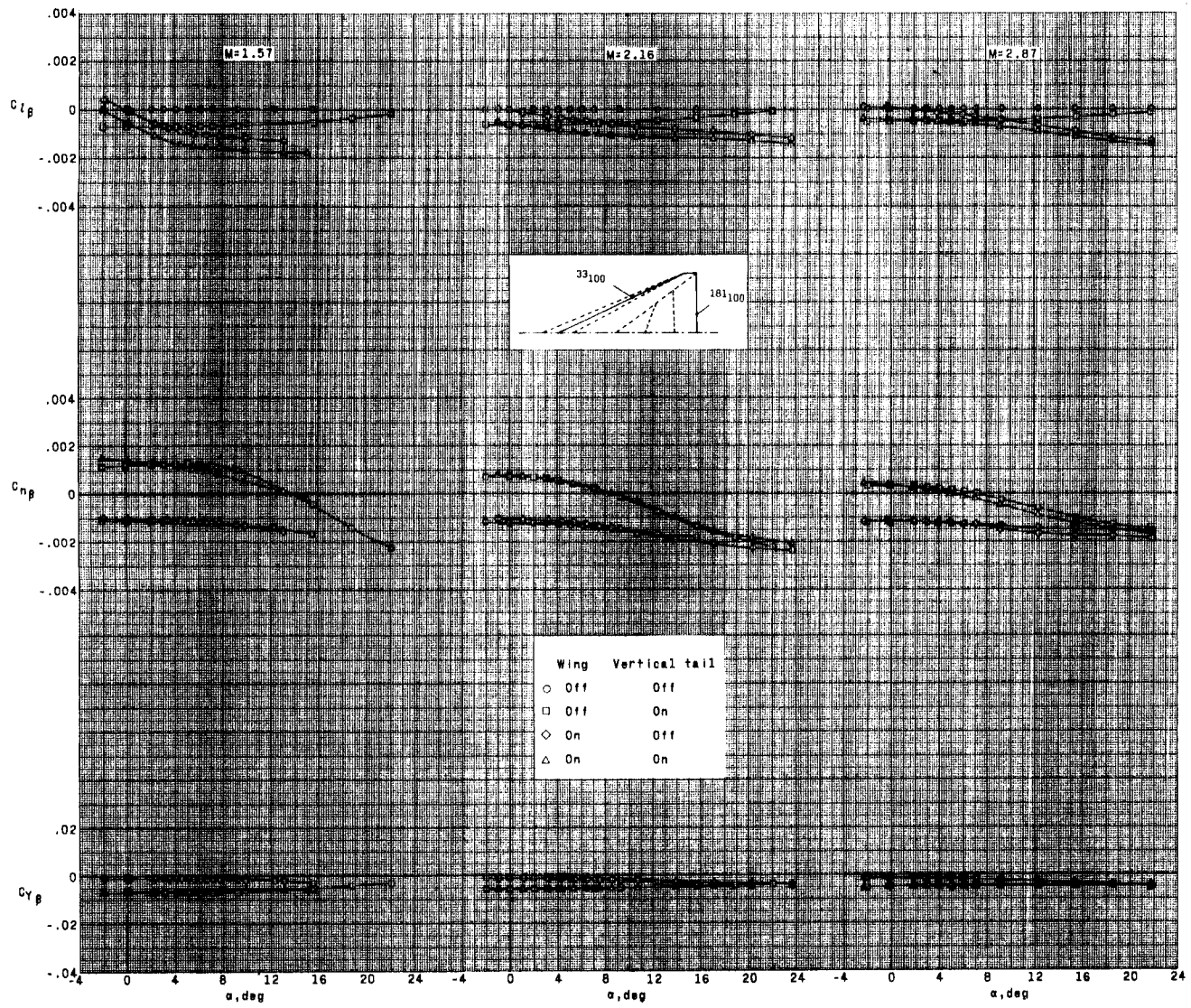

(h) 33_{100}-181_{100}.

Figure 7.- Continued.

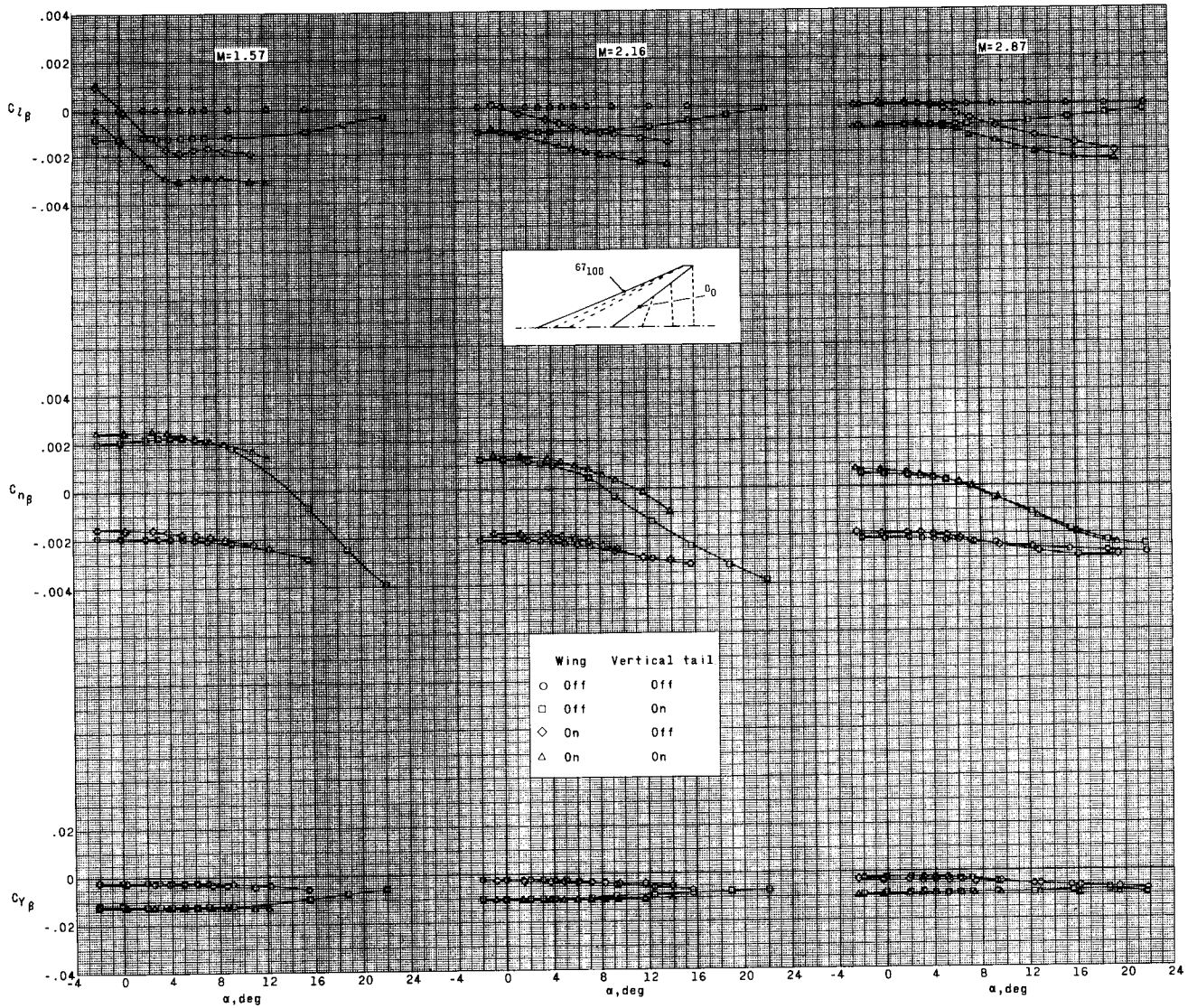

(i) 67_{100}-0_0.

Figure 7.- Continued.

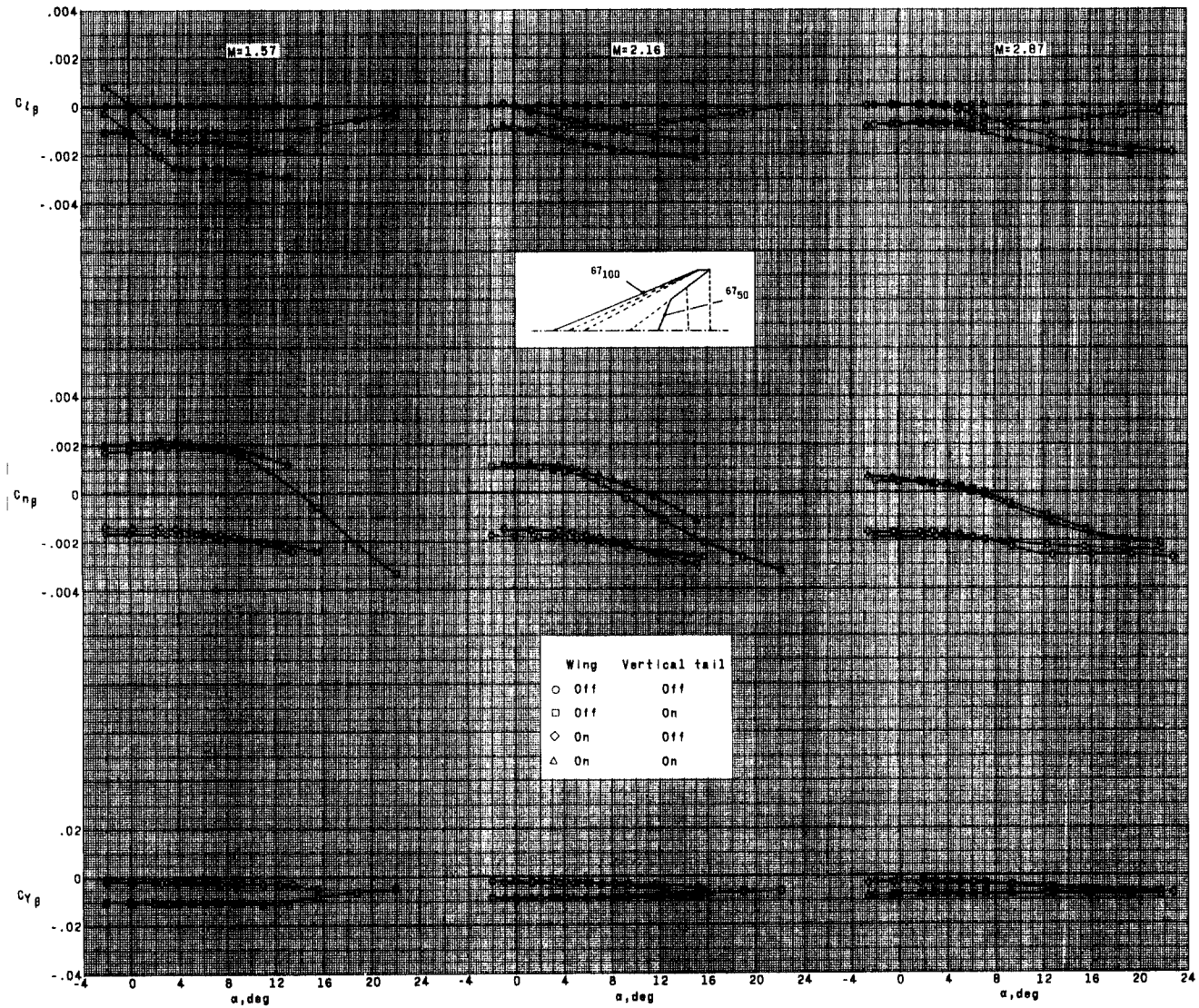

(j) 67_{100}-67_{50}.

Figure 7.- Continued.

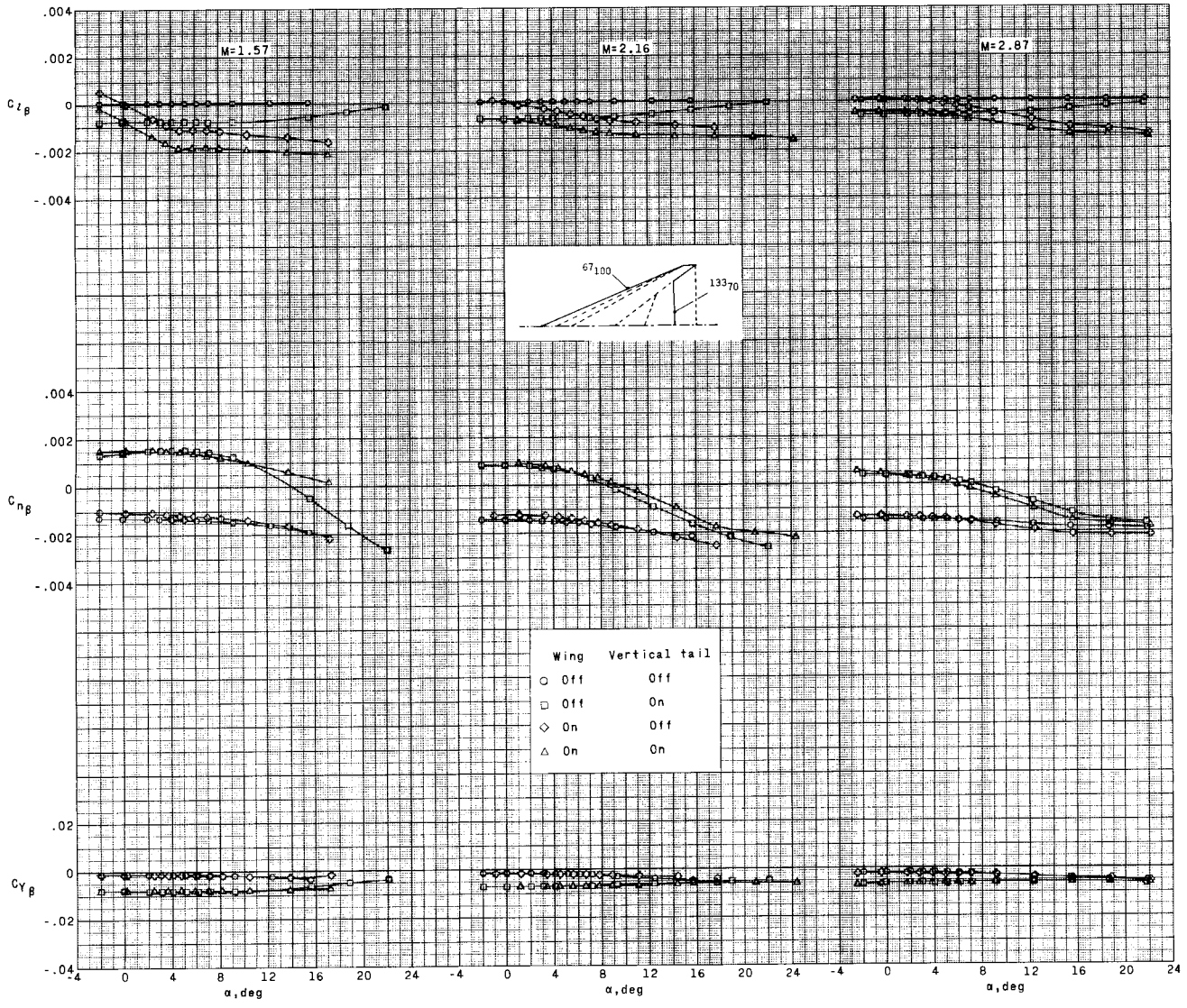

(k) 67_{100}-133_{70}.

Figure 7.- Continued.

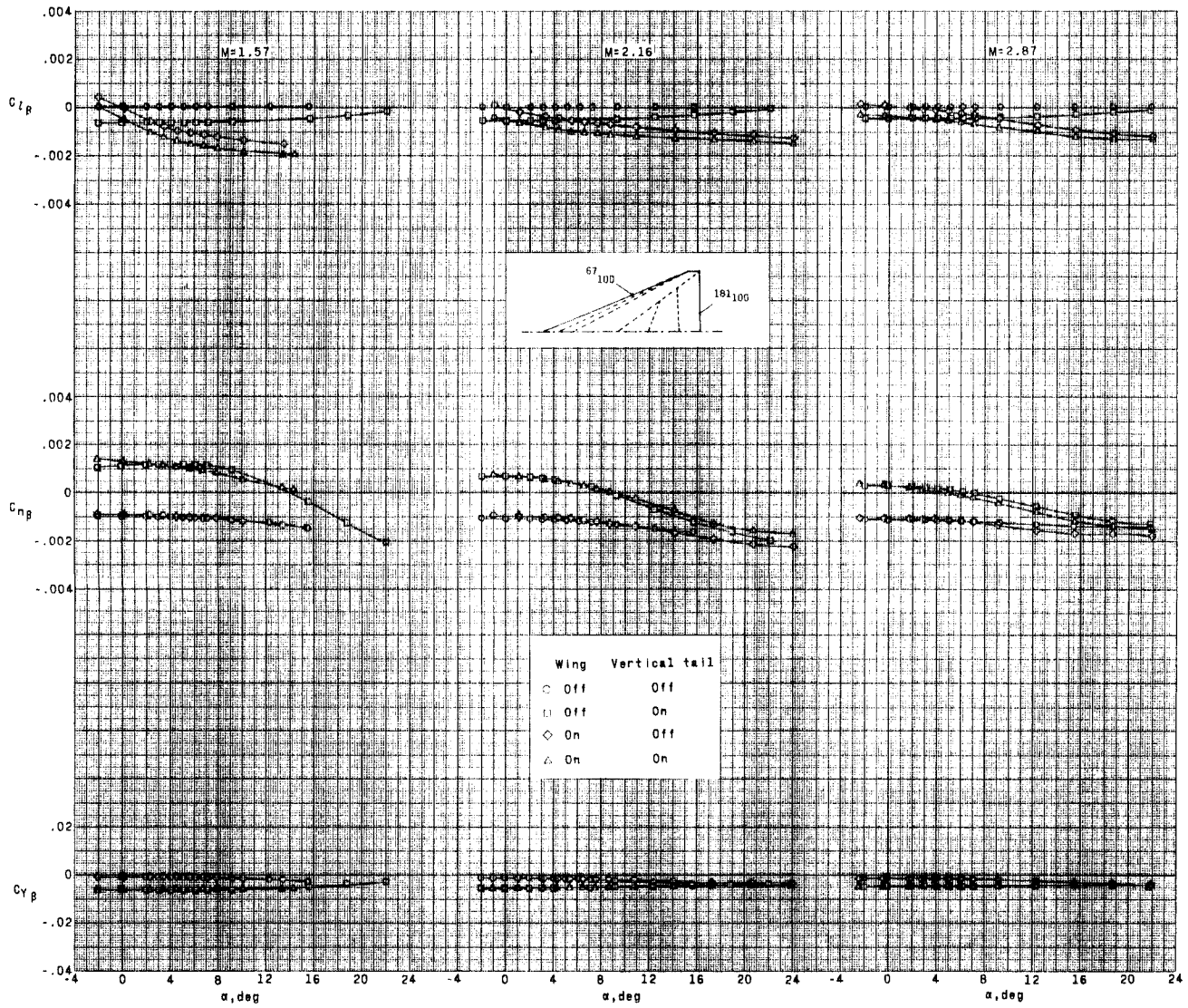

(l) 67_{100}-181_{100}.

Figure 7.- Concluded.

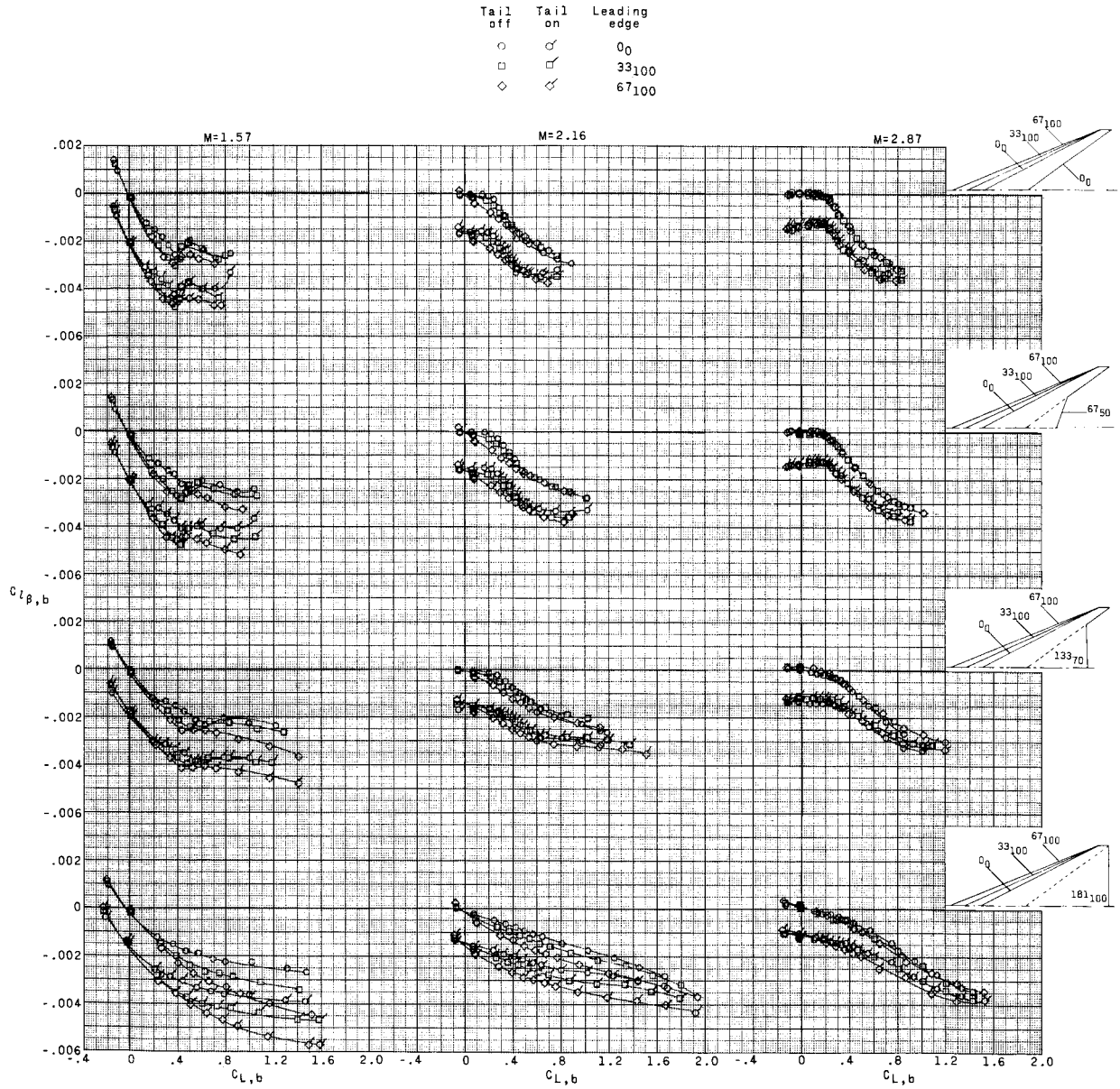

(a) Effective dihedral parameter.

Figure 8.- Effect of leading-edge modification on sideslip parameters. (Data based on basic wing area and referenced to model moment center.)

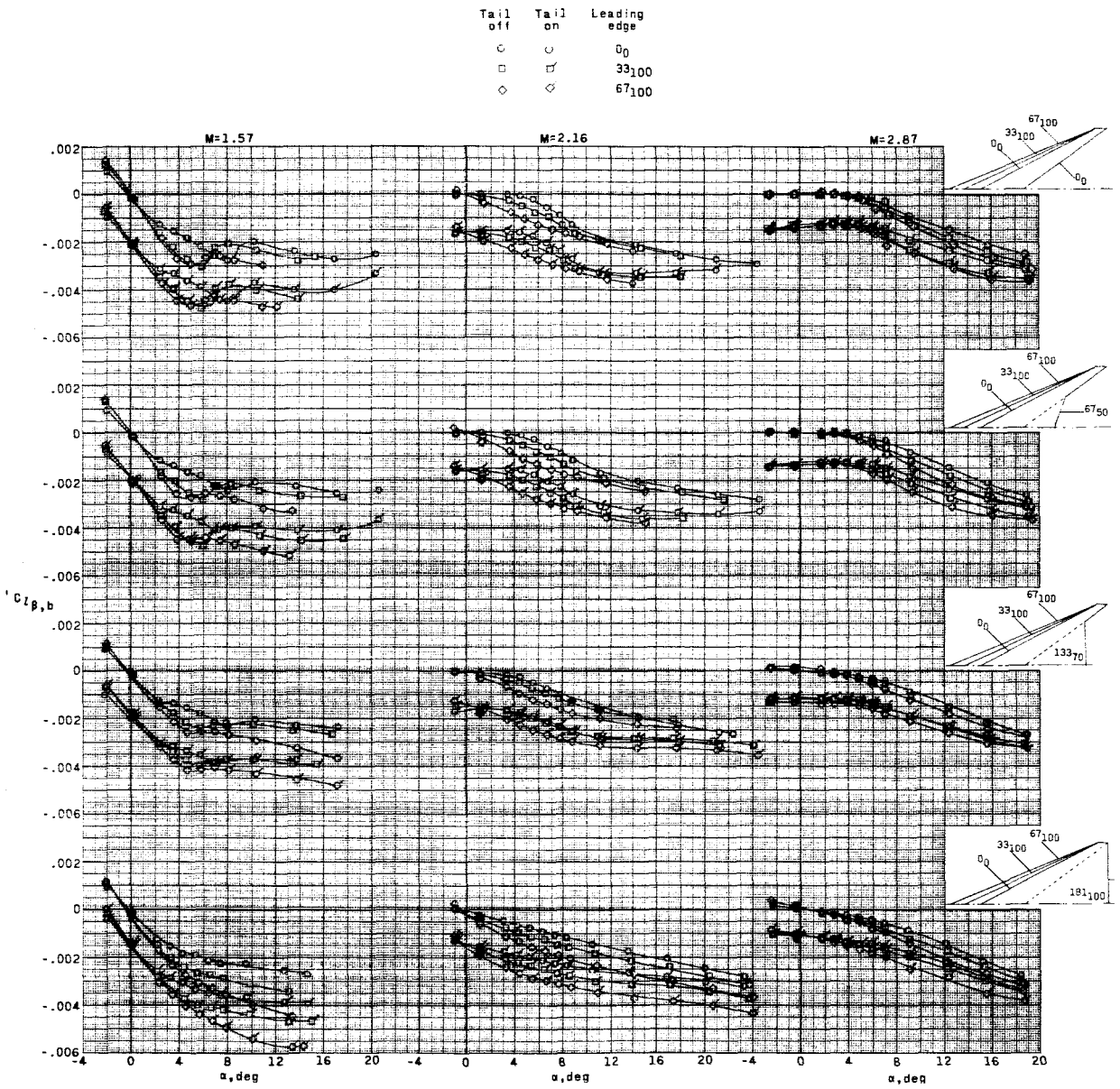

(a) Concluded.

Figure 8.- Continued.

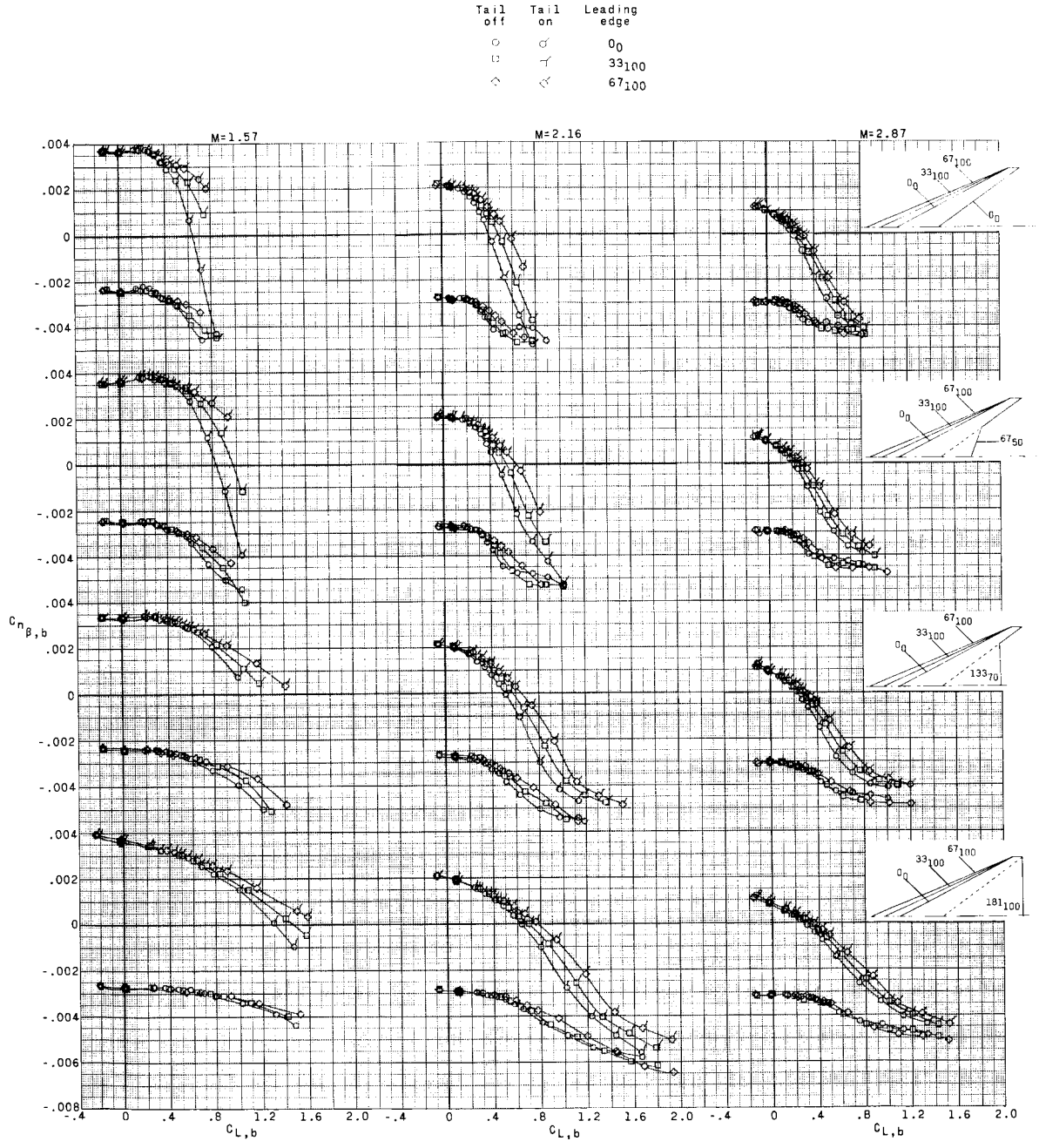

(b) Directional stability parameter.

Figure 8.- Continued.

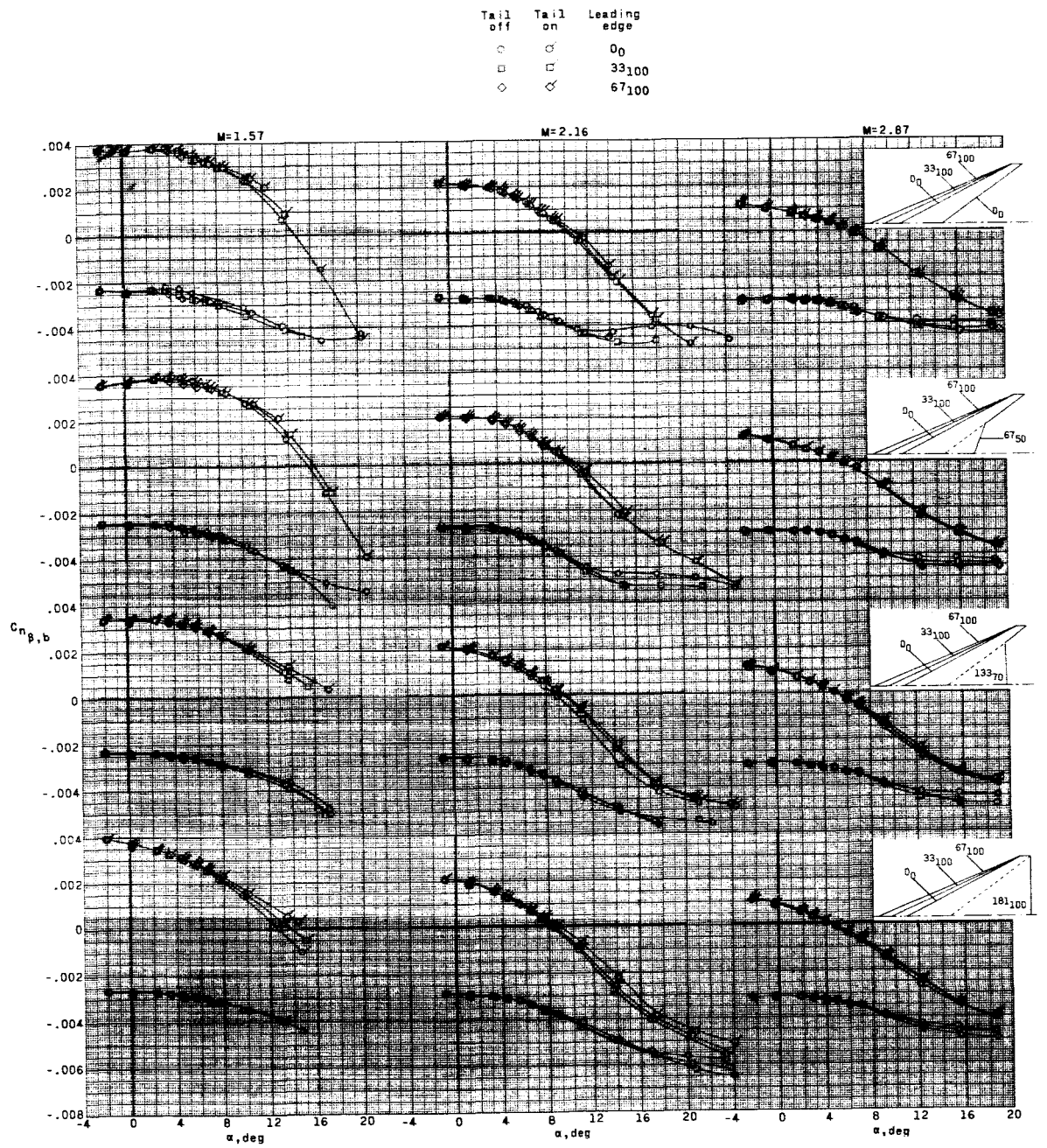

(b) Concluded.

Figure 8.- Concluded.

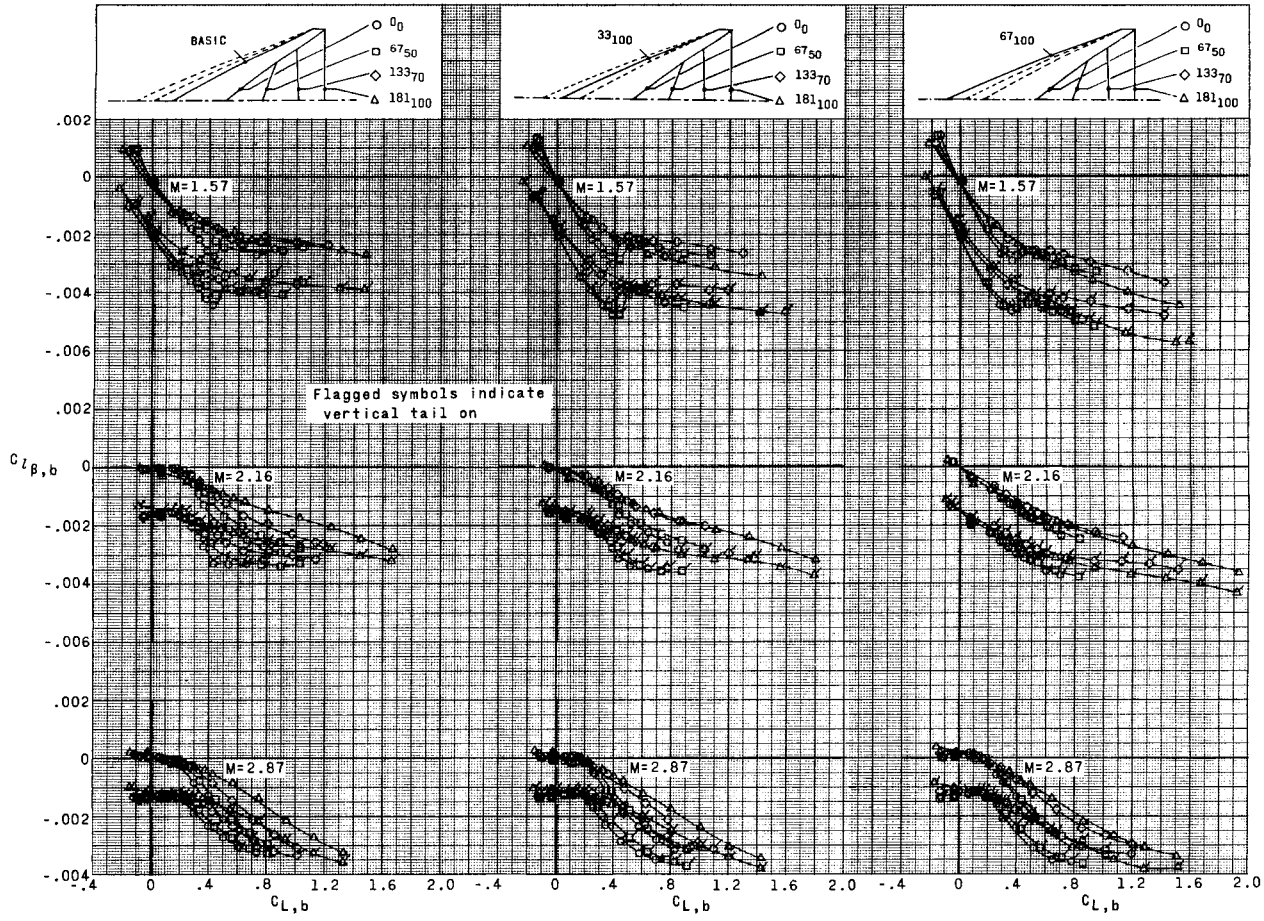

(a) Effective dihedral parameter.

Figure 9.- Effect of trailing-edge modification on sideslip parameters. (Data based on basic wing area and referenced to model moment center.)

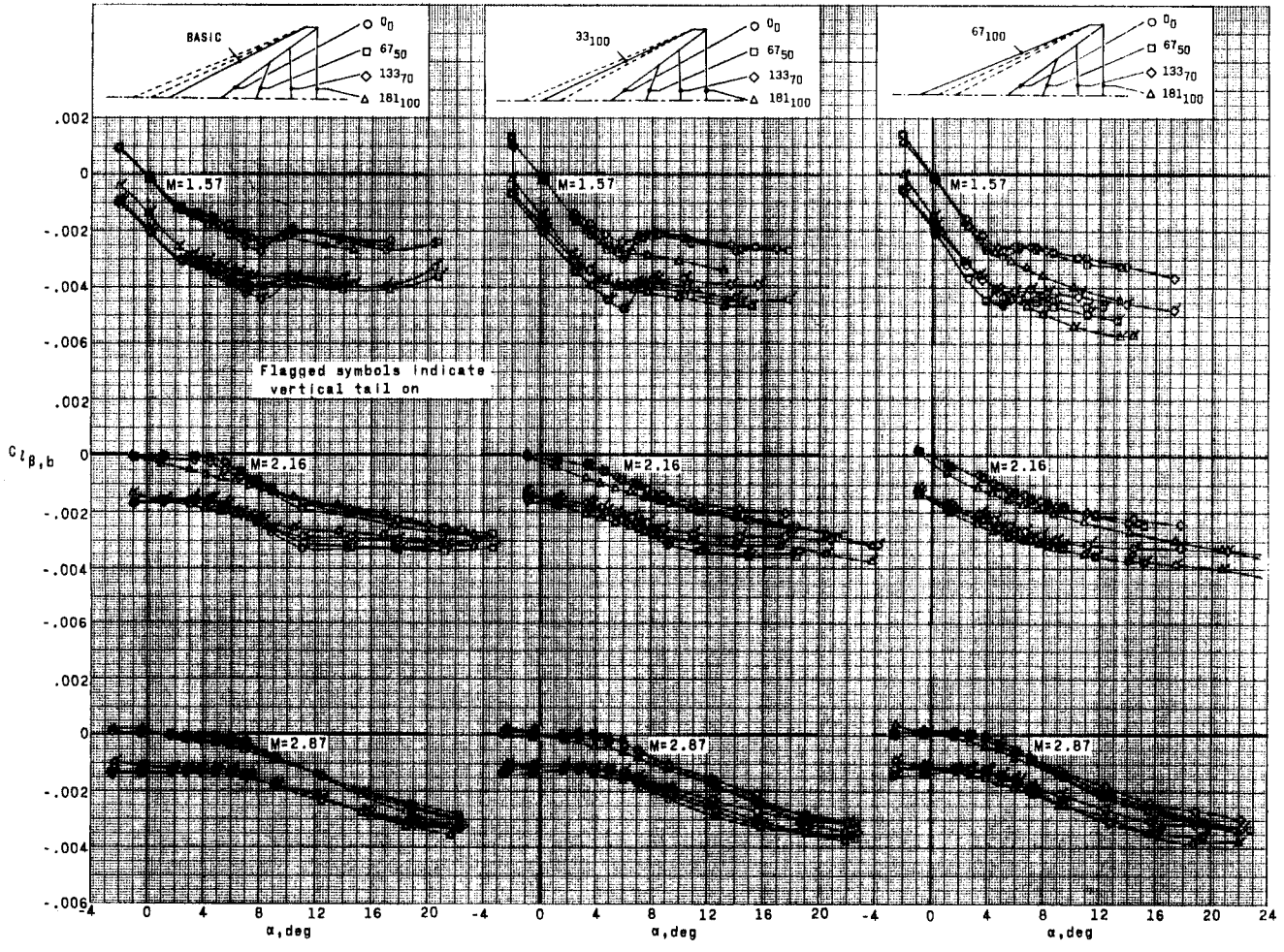

(a) Concluded.

Figure 9.- Continued.

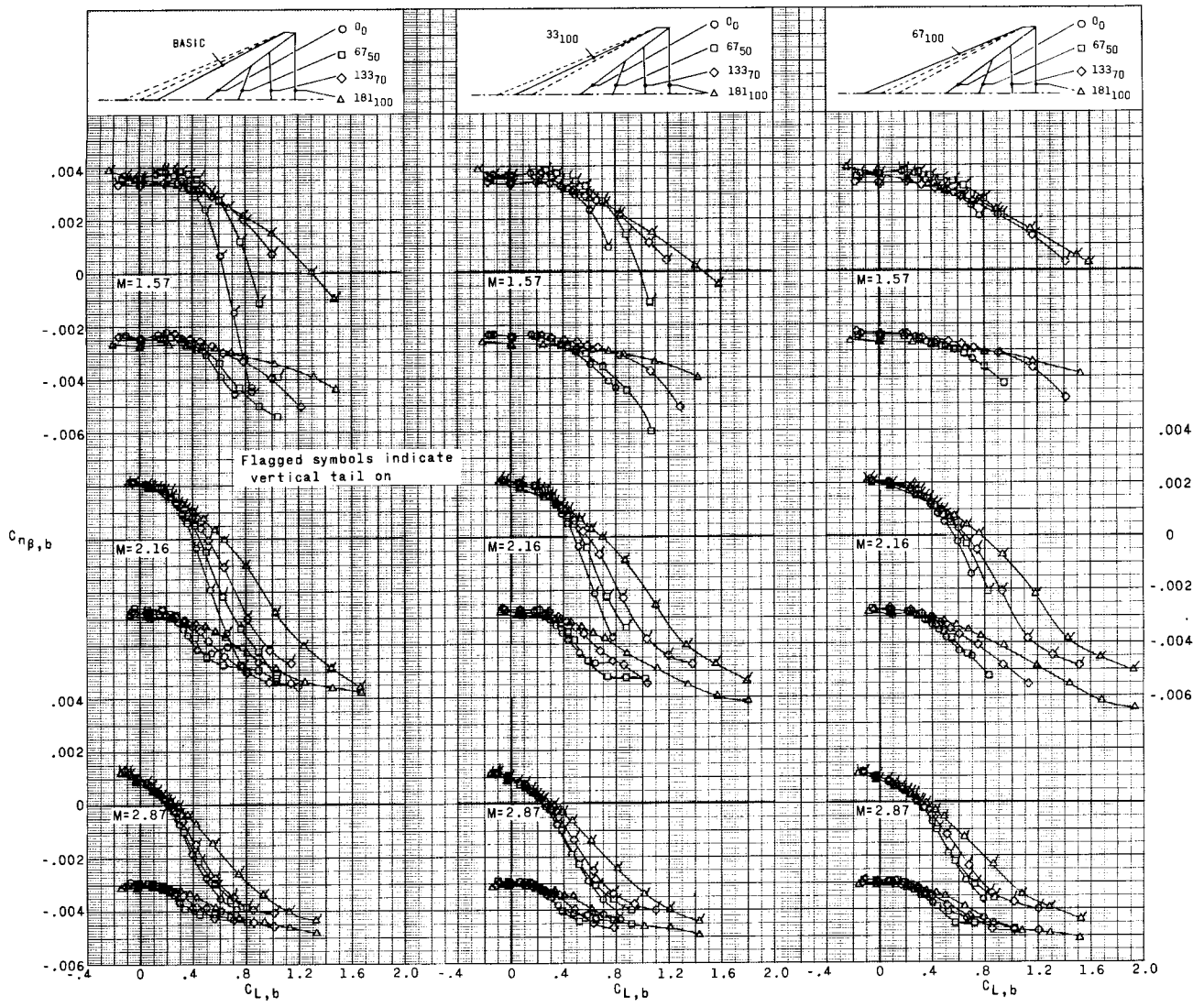

(b) Directional stability parameter.

Figure 9.- Continued.

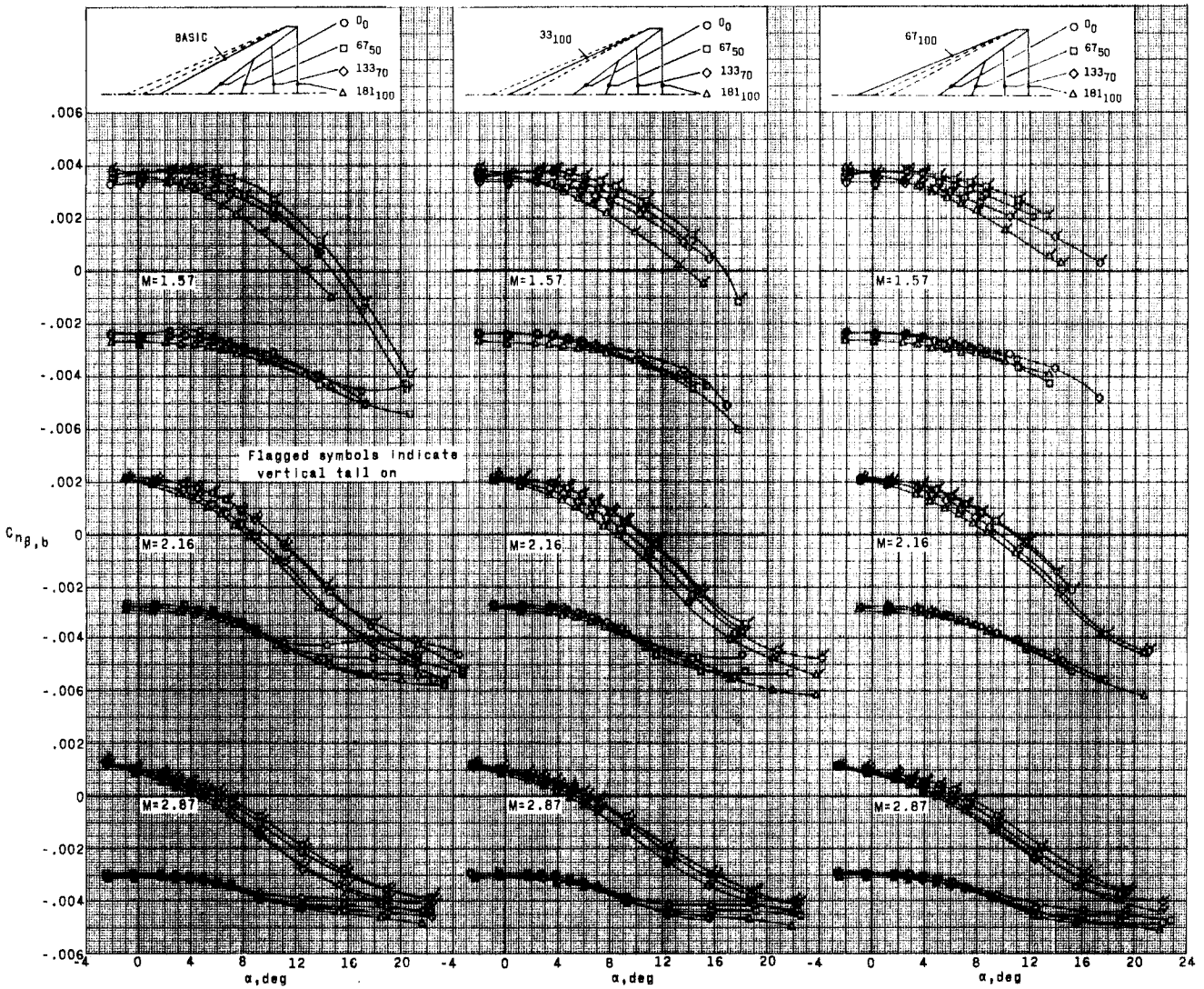

(b) Concluded.

Figure 9.- Concluded.

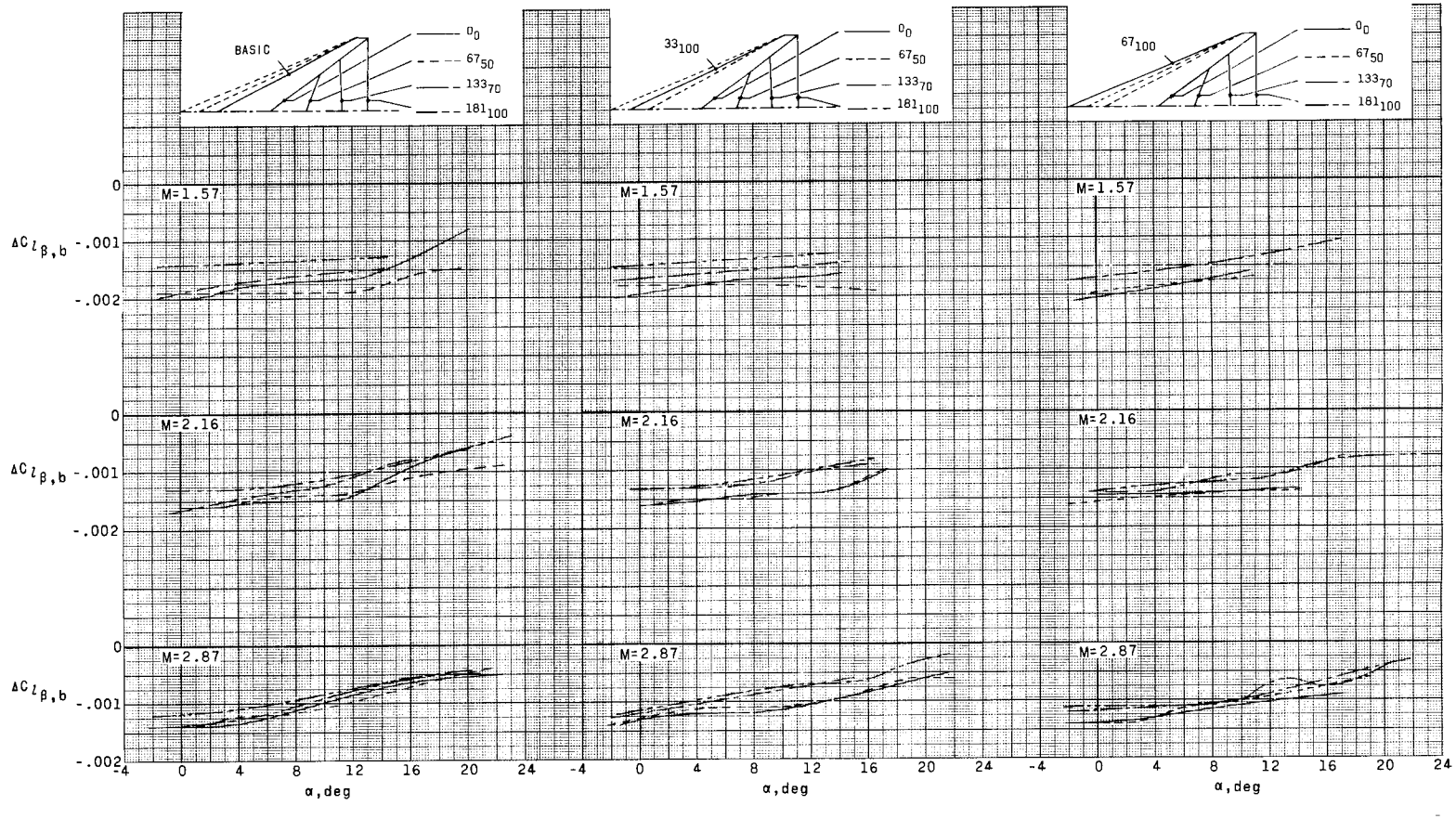

Figure 10.- Tail contribution to effective dihedral parameter. (Data based on basic wing area and referenced to model moment center.)

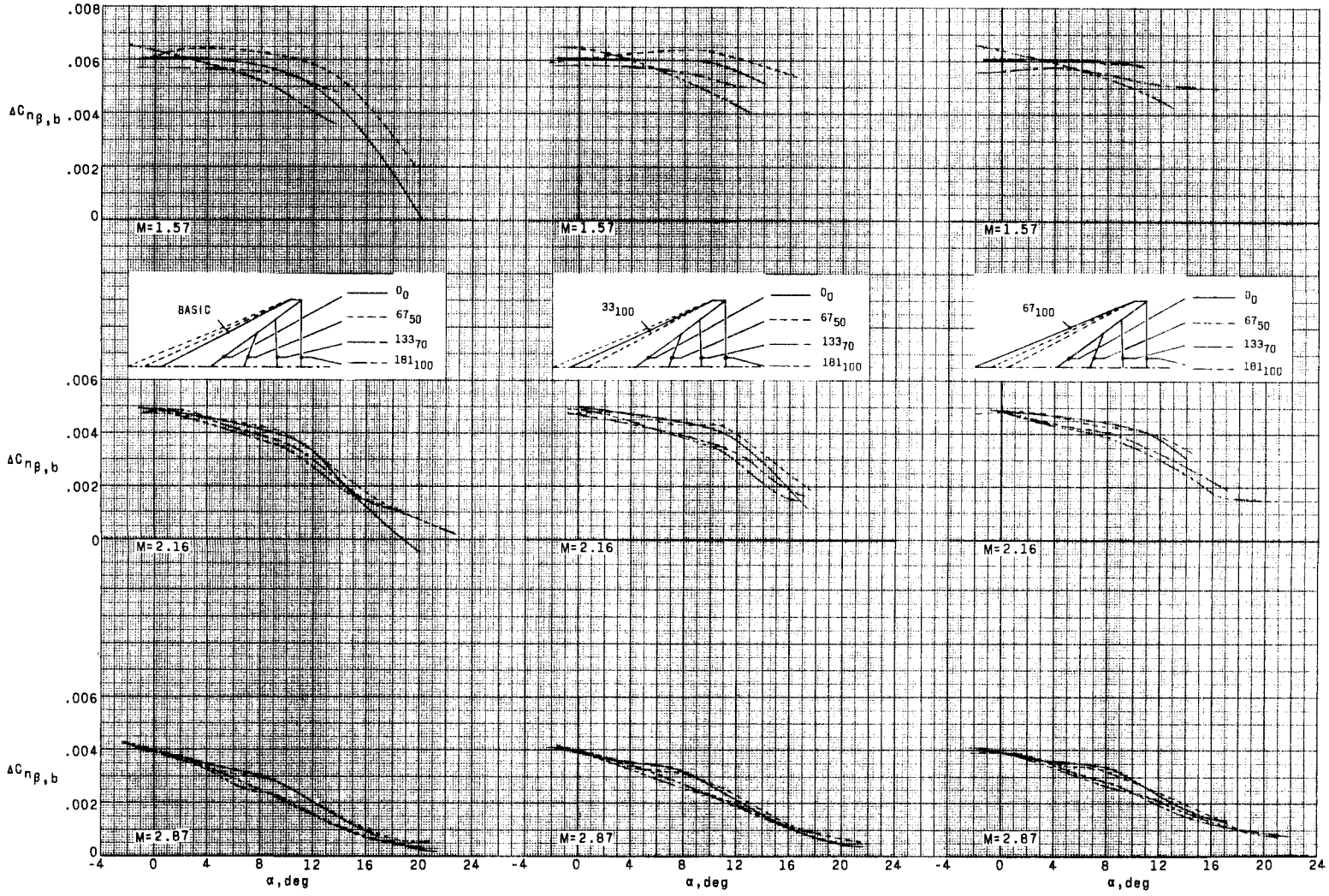

Figure 11.- Tail contribution to directional stability parameter. (Data based on basic wing area and referenced to model moment center.)

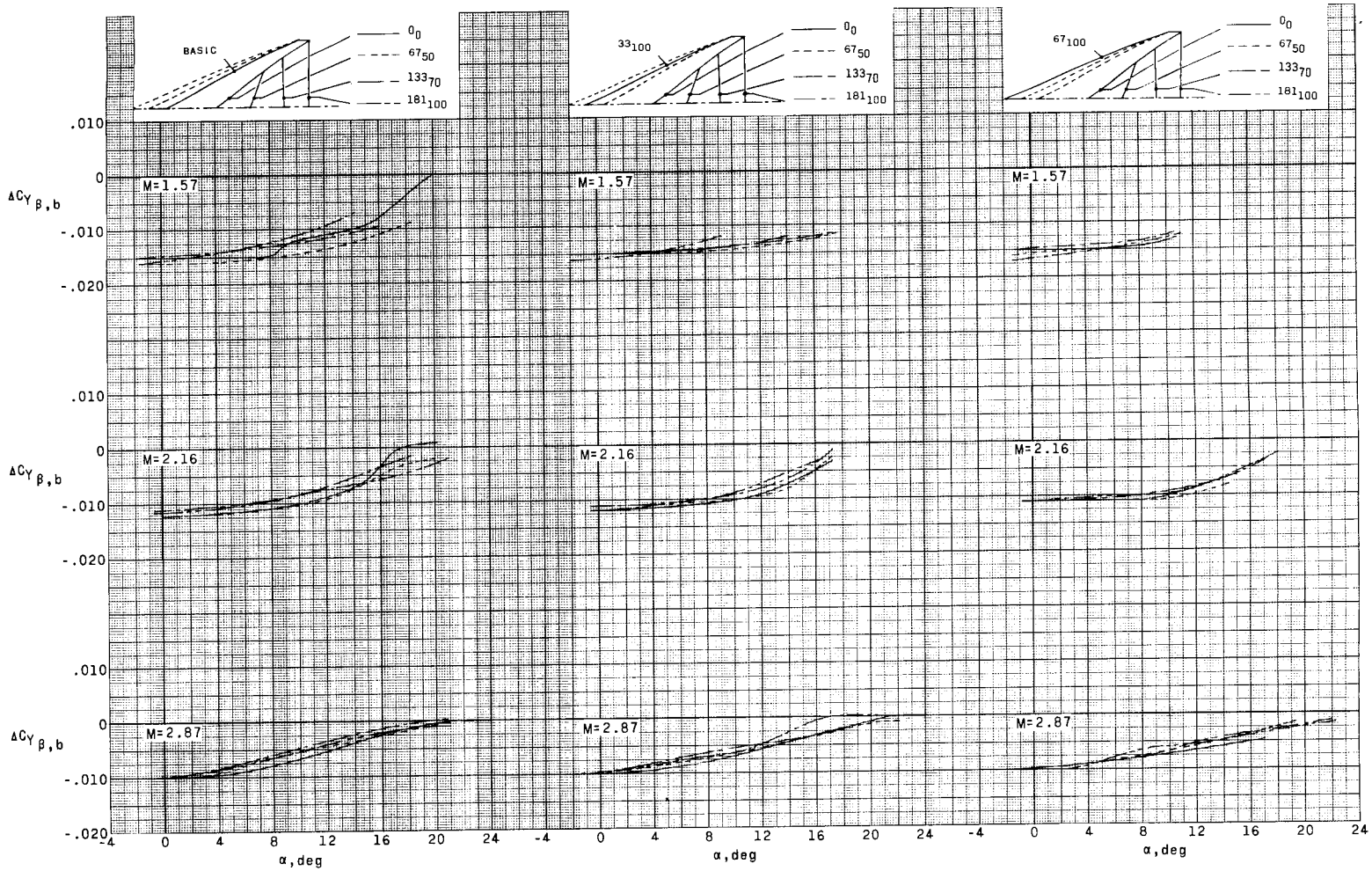

Figure 12.- Tail contribution to side-force parameter. (Data based on basic wing area and referenced to model moment center.)